学位申請論文

A computational and empirical study on blink synchronization induced by performer's inputs

(演者からの入力によって生じる瞬目同期に関する

計算論的・実証論的研究)

Ryota Nomura
Tokyo University of Science

March 2019

A computational and empirical study on
blink synchronization induced by performer's inputs
(演者からの入力によって生じる瞬目同期に関する計算論的・実証論的研究)

Abstract

Synchronization is one of the universal phenomena in the world and thus has been studied in a variety of fields such as physics, biology, and psychology. In recent years, blink synchronization in experiments with individual participants has been reported. However, it remains unrevealed that the nature of blink synchronizations in theatre where a performer and multiple audience members interact with each other. The purpose of this thesis is to explore the mechanisms of emerging blink synchronizations in theatre and its effects on human cognition and collective experiences by taking both computational and empirical approach.

In Chapter 1, I introduced the background of the research on blink synchronizations in theatre from the viewpoint of synchronizations as universal phenomena that are observed in a group of neurons as well as inter-personal interactions.

In Chapter 2, I discussed the conditions for emerging blink synchronizations in theatre. The possibility of emerging blink synchronizations depends on the degree of mastery of the performers. Moreover, higher subjective transportive experience was related to larger variance of inter-blink intervals (i.e., IBI). This result suggests that the professional performance leaded cognitive process regarding enjoyment while experts' act also guided the switching timing between attentional allocation and attentional shift. Subsequently, the blink rates change in accordance with the performance, leading to enlarge the differences between dense blinking and sparse blinking. Hence, the variance of IBI would be larger for participants who had much the transportive experience by the professional performance.

In Chapter 3, I explored the nature of blink synchronizations as a human collective behaviour. In a collective experiment under the theatre setting, the degree of blink synchronizations was increased $30 - 60$ % compared to that calculated using the data obtained in the laboratory experiment with individual participants, which was reported in Chapter 2. Regarding blink synchronization in theatre, collective viewing is highly more effective especially for the first-time viewers than the frequent viewers. Inter-

spectator forces, if I could refer to, influence attractively in collective viewing settings.

In Chapter 4, I proposed a mathematical model that explain human blinking focusing on the distributions of IBI. I discuss how the blinking patterns vary due to external inputs that is represented as the fluctuation of a threshold function. In particular, the model reproduced the previously known all four type of IBI distributions and the model also predict a trimodal IBI distributions that have not been reported empirically. The parameters of the model also suggested that relatively slow $(0.11 - 0.25[\mathrm{Hz}])$ oscillation governs the human spontaneous blinking.

In Chapter 5, I proposed that a method to reconstruct a time series of common input using overlapped multiple, i.e., superposed recurrence plots. The time series of the common input can be reconstructed based on superposed recurrence plots with high accuracy when the sufficiently high dimensional embedding and the widths of time window for calculating the firing rates were set to an effective value to capture the fluctuations of the common input. I therefore applied the method to the blinking rates as well. Using the superposed recurrence plots of audience members' blinking, a time series of the common input was reconstructed. The fluctuations of the reconstructed time series were assumed to be the common input of the expert performances that influence on blinking systems of audience members.

In Chapter 6, I discussed the blink synchronizations in theatre based on the numerical simulations and experiments in this thesis. Then, I stated the limitations of this study and possible interpretations. Finally, I referred to the remained problems and future research on the theatre communications.

Contents

List of Figures

List of Tables

Chapter 1

General Introduction

Synchronization is one of the universal nonlinear phenomena in the world. In physical systems, more than two oscillators entrain each other, resulting a unitary paced motion. For instance, two metronomes that beat a steady rhythm can synchronize each other if they are put on a movable plate, even when their pendulums are initially set to different angles [5], [6]. Biological systems are also dominated by a variety of synchronization. In microscopic level, for examples synchronization in neurons [7] enables human critical activities such as recognition, reasoning, and emotional expressions. As an interpersonal aspect, motor synchronizations [8] and contagions of physiological behaviours, e.g., yawing, smiling, and laughing [9], may serve as the core component of empathetic system of human as a social animal [10].

In 2009, Nakano and her colleagues [11] reported "eyeblink synchronization" of human. In this experiment, participants were individually presented comedy movie 'Mr. Bean' in a separated laboratory. As the results, the spontaneous blinking tended to occur in particular time bins, i.e., participants tend to blink at particular frames of the film, showing a synchronized blinking among participants. The frames of increasing blinks included implicit breakpoints inferred of the story line as well as explicit breakpoints. Although this phenomenon could be referred as a "blink increase" at particular scenes, Nakano et al. named as "eyeblink synchronization." Based on a deductive speculation, some researchers may assume that audience members in theatre would blink at similar timing as well. In theatre, however, many factors are involved in interactions between a performer and a number of audience members. Theoretical and numerical researches in the field of physics have revealed that synchronizations are

induced by a common input (e.g., pulse [12] and noise [13]). When the oscillators are mutually coupled [12], however, synchronizations are not maintained without refractoriness to influences by the other oscillator. Consequently, in some cases, the coupled oscillators desynchronize due to the interactions between oscillators. Hence, whether or not blinks synchronize among audience in theatre is a non-trivial problem.

Despite the long history of empirical researches on human blinking, there exist very few computational models to represent the behaviour of human spontaneous blinking per se, before the examinations of the considerations of blink synchronizations. Numerous empirical studies have revealed that human blink rates vary depending on cognitive load and task-demands. In theatre as well, psychological variables such as cognitive load would constantly fluctuate on the order of $100 - 10,000$ [ms] while each individual is viewing theatre performances, resulting in a variety of blink intervals. And therefore, it is necessary for researcher to develop a model that explains these temporal changes in blinking patterns. Primarily, it is not understood that the conditions of emerging blink synchronizations in theatre. Secondary, even if blink synchronizations surely emerge in theatre, it remains unclear how the phenomenon influence human cognition and experience processing. If we obtain fundamental understanding in blink synchronizations in theatre, researchers could know their important roles in the relation to particular performer-audience communication as well as interactions among audience.

Chapter 2

Blink Synchronization in vaudeville settings and its psychological influences

To my best knowledge, blink synchronization in theatre has not been a theme of scientific research. After the observation of blink synchronization in theatre in 2013 [3], I have been studied blink synchronization which reflect attentions process during viewing the performance with using Raking which is a Japanese traditional story-telling performance. To verify the mechanism of blink synchronization, I exerted an experiment with individual participant who are not familiar with Raking performance and examined whether or not blink synchronization occur more frequently during viewing a video that performed by a expert actor than that by a novice actor.

First, the results demonstrated that blink synchronization occurs among participants who are not familiar with Rakugo performance. The audience would be difficult to make the storyline in long-term prediction. Thus, the results suggest that blink synchronization does not depends on the prior knowledge. Then, the results also showed that blink synchronization is observed in the situation where there exists no laughter. Therefore, blink synchronization does not need laughter of other audience members as the primary condition. Next, the timing of blink synchronization is unrelated to actor's blinks, and therefore blinks synchronization is not a byproduct of blink entrainment between an actor and each audience member. Finally, the timing of blink synchronization related to important scenes to enjoy the story. The results suggest

that expressive contents lead particular temporal patterns in attentional cycle. Addition to this, the frequency and degrees of blink synchronizations corresponded to expertising levels of actors who performed the same story. Hence, we would conclude that blink synchronization occurs due to expressive contents rather than the structure of the story.

In the study ([3], Study 2), the participants who were not familiar with Rakugo performance were selected for detecting the minimum conditions for blink synchronization. However, the viewing skill of audience members can change through the repetitive appreciation. There are both possibilities that the prior knowledge of the actor and the story leads to be easier to occur blink synchronization by providing the common framework and such knowledge leads to be more difficult to occur blink synchronization by building original value standard for appreciation.

Collective spectator communications such as oral presentations, movies, and storytelling performances are ubiquitous in human culture. Spectators who share time and space frequently involve their minds and bodies in fascinating performances. Some spectators would describe their experience as being 'carried away by the story. This engrossing temporal experience is known as "transportation into the narrative world" [14]. In a previous study, researchers summarized facilitators of narrative transportation [15]. For instance, van Laer et al. [15] pointed out that stories containing more identifiable characters to audience members, plotlines that storytelling audiences can imagine, and verisimilitude all increase the likelihood that a narrative transportation will occur (p. 803). In addition, an audience member's familiarity with a story topic, attention level, transportability (i.e., "a story receiver's chronic propensity to be transported," see Ref. [15], age, education, and gender (female rather than male) all play a role in the likelihood of narrative transportation (p. 804). Although these studies have focused on human traits, in other words, static factors of transportation, dynamic factors such as fluctuation between attention allocation and attention release during a performance also affect a transportive experience in live theatre, as expressiveness between a performer and the audience is communicated in real-time. However, the processing mechanism by which an audience experiences transportation through the appreciation of expert performances remains a mystery.

Investigations into audiences' transportive experience during a storytelling performance have suggested that audience attention tends to synchronize with the addition

of audio-visual stimuli used during expert performances [3]. In Ref. [3], Nomura and Okada showed that during an expert performance, eyeblinks among participant audience members synchronized with greater frequency and more intensity compared to audience members of a novice performance, even though the expert and novice performers performed the same story. At the same time, subjective rating scores on a scale to determine transportation into the world of the story [16] including somatic responses (e.g., sweat and chills, [17] were much higher for participants who watched an expert performance than those who watched a novice performance.

The timing of eyeblinks is interrelated within attentional process [11] [3]. In general, people search for a target upon which to focus their attention. If audiences find a target, they allocate their attention to it. After this focused concentration, they release their attention to prepare to search for the next target. Audience eyeblinks decrease at the moment of attention allocation while they increase at the moment of attention release. Therefore, eyeblinks tend to synchronously occur at implicit attentional breakpoints among readers while reading books [18] and among viewers while viewing videos [19]. An additional qualitative analysis in Ref. [3](Study 2) also indicated that eyeblinks among audiences are synchronized corresponding to scene changes and high points of expressive performance. This externally coordinated attention leads to an efficient cognitive process by avoiding loss of significant information [11]. Thus, the authors concluded that eyeblink synchronization among audiences is guided by an expert performance created to make audiences comprehend the important information.

However, it is unclear how eyeblink synchronization among audiences relates to their experience of transportation. One of the possible mechanisms is that eyeblink synchronization among audiences is driven by attentional cycles, which are in turn driven by emotional processing. One's eyeblinks usually cycle in self-paced (physiological) periods with some fluctuations. However, audience eyeblink onset might be delayed or accelerated depending on the actors' expressions, as the timing of attention allocation and attention release are coordinated with the performance. When audience members shift their attention back and forth more frequently, in parallel with the storyline and punchlines performed by the actors, eyeblink time points vary dynamically, but sensitively, in line with the performance [3]. As s result, eyeblinks among audiences synchronize with each other. Because the duration of attentional cycles reflects the audience's active involvement in a performance, durations vary more frequently

than those of self-paced cycles. Such dynamic attention shifts bring audience members more emotional excitement. Their emotional excitement may motivate them to pay attention for upcoming expressions that could contain important content-related information. Thus, a reciprocal process between emotional excitement and the resulting motivated attention would affect transportative experiences. In other words, high emotional excitement and high eyeblink variability would predict that audience members experience more transportation.

The other possibility is that a situation model improves prediction accuracy and simultaneously facilitates the experience of transportation. A situation model refers to a reader's representation of the referents and events described in a text [20]. More generally, it refers to a story receiver's mental model [21] using specific information that aids the comprehension of the current situation. When people comprehend a story, they construct a representation of the situation and its words and sentences [22]. The current situation model manages new information from the aspect of temporal, spatial, or casual consistency [23] and possibly enables people to predict the next plot twist more precisely. If an audience can construct representations of a story, they will more easily understand the meaning of the situation. In other words, a situation model reduces the cognitive burden required to comprehend a story. At the same time, this reduction facilitates the experience of transportation, because audiences can freely use remaining cognitive resources for other cognitive activities, such as focusing on the detail of expressions. Thus, a model can help an audience realize the depth of feelings expressed in a performance. While a non-experienced audience constructs a situation model by using only the knowledge accumulated through appreciation of the present story, an experienced audience constructs a model by also exploiting domain knowledge cultivated through past viewing experience. In light of this perspective, it could be predicted that the experienced audience, compared to the non-experienced audience, would gain more transportative experience from the beginning of a performance.

In summary, the mechanisms of audiences' blink synchronization reflecting the experience of transportation are as follows. On one hand, externally coordinated attention leads to dynamic eyeblink shifting, as well as emotional processing, due to which audience members are inclined to pay additional attention to the performance. On the other hand, a mental model reduces the cognitive burden of comprehending characters and plotlines of a story, while simultaneously improving the accuracy of prediction.

These two mechanisms facilitate audience eyeblink synchronization. However, these mechanisms could be interdependent. In general, synchronizations caused by external inputs are possible if respective elements respond reliably to time-varying stimuli [24]. Thus, blink synchronization among audiences during Rakugo settings could occur owing to performance quality in addition to audience sensitivity to external stimulus. For instance, even though emotional excitement and biased distribution of eyeblinks predict the transportive experience, this result may be obtained from the experienced audiences only if domain knowledge is a necessary condition. In another case, even the non-experienced audiences may obtain a transportive experience if the performance contains sufficient information to guide their attentional process. The purpose of this study is to examine these two potential mechanisms and their relationship to each other. In the experiment, experienced and non-experienced audiences were assigned to watch one of two videos separately: an orthodox performance (played in front of frequent viewers) or a modified performance (played in front of first-time viewers) acted by the same artist (The details of the two performances will be described later). In all settings, participants' eyeblink responses were observed.

The time cycle of inter-blink intervals (IBIs) varies when the performance contains more frequent expressions that draw the viewer's attention, because the original (self-paced) period becomes accelerated or delayed. This leads to a higher rate of eyeblink variability. Thus, the standard deviation of IBIs can be used as a measurement of eyeblink-rate variability on an individual level. Furthermore, emotional excitement can be measured by a subjective rating score on a humor scale, while it is no simple task to measure each audience member's situation model per se during real-time processing. However, the similarity of situation models among audiences could be estimated by focusing on the reproducibility of participants' eyeblink responses, because eyeblinks by audiences who have a common situation model would unintentionally select similar information, leading to more closely-timed (i.e., more reliable) and more similar eyeblink patterns. In this study, we observed the precision of eyeblink responses by focusing on time differences within an audience, instead of defining the objective criteria or identifying audio-visual information to which an audience allocates its attention. We calculated mean eyeblink timing asynchrony and estimated mean similarity of IBI patterns between two particular audience members as group-level indices of reproducibility.

To investigate the first mechanism, we performed a multiple regression analysis with a standard deviation of IBIs and humor ratings as an explanatory variable with a self-reported degree of transportation as a target variable. This hypothetical mechanism is rejected when standard deviations of IBIs or a subjective-humor response have no predictive power. Here, we were unable to eliminate the possibility that other variables suggested by previous research (van Lear et al., 2014) were also facilitating or inhibiting the process interdependently. In the multiple regression analysis, we included age, gender, mean of IBIs calculated for each individual, knowledge of the performer (a dummy variable), and knowledge of the story (a dummy variable) as possible predicting variables. This analysis was performed across the experimental conditions, with the aim of determining whether variables of real-time processing, rather than other variables such as the nature of performance or the different viewing experiences, had a predictive power for transportive experience. As the first hypothetical mechanism was supported by multiple regression analysis, we went on to examine the second mechanism, concerning the use of a situation model. If the asynchrony of eyeblinks was lower in the experienced audience group than in the non-experienced group, it would suggest that domain knowledge had helped in the construction of a situation model. One-way ANOVA was performed to assess the interaction between viewing experience and actor expression during performance. If a situation model was unnecessary for transportation, the degree of transportation did not increase, at least in the situation in which group-level eyeblink asynchrony was high. If any other factor was suspected of contributing to the process of transportation throughout the analyses, an additional analysis was performed according to the nature of stimuli such as laughter of audience recorded during Rakugo (Japanese) vaudeville performances (i.e., in situ).

2.1 Materials and methods

2.1.1 Participants

Participants included 28 males and 44 females, all native Japanese speakers. Out of 72 people who participated in the experiments, complete eye-tracking data was obtained from 60 participants (24 males and 36 females, mean age = 34.12 yrs., range = 18−−63 yrs.). Eye-movement data from two people was not usable due to drooping eyelids.

Data from 10 other people were unusable because troubles with the instruments caused a loss of eye-detecting information leading to insufficient records. The experimenter defined participants who had viewed the type of storytelling performance used in the study more than ten times in any situation, including through other media and live performances, as an experienced audience member. The experimenter adopted the criteria because the mean number of viewing times was usually three or four times in the daily lives of most Japanese. This meant that individuals who met the criteria seemed to seek opportunities to view Rakugo more than five times. As a result, 30 (15 experienced and 15 non-experienced) participants were assigned the videotaped performance as first-time viewers and the remaining 30 participants (15 experienced and 15 non-experienced) were assigned the videotaped performance as frequent viewers.

2.1.2 The storytelling artist and stimuli

In the current study, the authors asked professional Rakugo artist Bungiku Kokontei (34-year-old performer with 10 years' experience) to record his performances. Rakugo is a traditional Japanese comic vaudeville storytelling performance in which one artist plays many characters. The stage setting is usually just a square cushion (zabuton) on which the performer sits to tell passed-down and newly created stories. The artist uses a Japanese fan and a traditional hand towel to represent all stage properties such as chopsticks and a sword (katana). In a traditional Rakugo apprenticeship of the Association of Rakugo (General Incorporated Associations), the title of first-rank performer ("Shin'uchi") was given to Bungiku earlier than the 28 senior performers. We therefore assumed that Bungiku possesses the skills to modify his performance according to the nature of the audience. Two storytelling performances as well as the audio-visual information during the performance were videotaped. In both performances, the story Bungiku told was called "Nibansenji," literally meaning the second brew of tea or decoction, which is semantically transferred to mean that things become a pale imitation. The outline of the story is as follows: five civilians go around the city of Edo (the old name of Tokyo) to prevent fires on a very cold winter night. After enduring the cold, they go back to a hut and have a warm meal, while passing around a small cup of warmed sake, conveniently concealed as "senji-kusuri" (decoction). Suddenly, a samurai who supervises the fire-prevention activities comes to the hut and calls for the door to be opened. Although civilians hurriedly hide the meal and sake, the samurai

notices them quickly and wants to make them his own, relying on his authority. While the samurai wants another decoction (i.e., sake), one of the civilians answers that they have no more decoction. As the last line, the samurai orders as follows: "While I patrol around the neighborhood, brew the second decoction."

The performances were recorded on December 6th, 2013, in a Rakugo vaudeville setting that was recreated in a laboratory room at the University of Tokyo. The artist performed live in front of 31 frequent viewers and 24 first-time viewers. They (i.e., audience in situ) were different from participants of the current laboratory experiment. Several experimenters and assistants were also present in the room. The performance for frequent viewers was acted in the style of traditional vaudeville storytelling performance in everyday theatre (orthodox video). The performance for first-time viewers was played in a modified way to help first-time viewers better comprehend the content of the story (modified video). The videos lasted approximately 3220 s (53 min 40 s) and 3022 s (50 min 22 s), respectively. For the first-time viewers, the artist took a few minutes to explain the traditional way of viewing this type of storytelling performance.

The videotaped performance was presented on a 19-inch monitor distanced 58 cm from each participant. The video was projected to a size of 15 cm (H) $\times$ 24.6 cm (W). The subjects' viewing angle of the performer, who was sitting on the zabuton, was approximately 11.3 deg $\times$ 10.7 deg located at the center of the monitor. The projected size was approximately equivalent to the size of performers viewed by an audience seated at a 5-meter distance in the center of a vaudeville theatre. The video stimuli were controlled by a desktop personal computer (Dell, Optilex 900, CPU 3.40 GHz, Memory 8.00GB).

Eye movements were measured by a non-contact, eye-tracking device (EMR-AT, VOXER, nac Image Technology Inc.) at a sampling rate of 60 [Hz]. The eye position was smoothed using a moving-average method and recorded electronically. The eyeblinks were detected by instantaneous losses ($0.3-1.0$ [s]) of pupil with an eye-position motion that went rapidly down and then immediately up. The first time point during the detected eyeblink was identified as the onset of that eyeblink. The time duration from one onset to the next onset was defined as the IBI. Each participant's chin and forehead were placed in fixed way on a support device to minimize the influence of head movements on eye-tracking data. Presentation of stimuli were controlled and recorded by a background program made by Visual Basic. A few time delays occurred before the

presentation while the computer was loading a video. These presentation time delays were corrected using recorded time stamps.

2.1.3 Questionnaire

The questionnaire package consisted of two scales (humor and transportation), two demographic characteristics (age and gender), and domain knowledge of the storytelling performance being shown. Humor as the emotional excitation in vaudeville settings was rated using a 4-point (from 1 to 4) Likert scale. The humor rating scale [25] included four items that reflected the audience's degree of perceived humor (e.g., "I laughed or was inclined to laugh so much"). The transportive experience was rated using 18 items related to temporal transportation. Half of the items were derived from a subscale of the Literary Response Questionnaire (LRQ, [16], which was translated into Japanese [26]). However, the wording of questions was inverted to fit into a vaudeville setting. For instance, "reading a novel" in the original text was changed to "viewing Rakugo" in the modified text [17]. The translated questionnaire also contained items relevant to the emotion of enjoyment in real life or items relevant to the author of the stories rather than transportation per se and less relevant items, which were not used. Moreover, as another aspect of the transportive experience, some items reflected subjective evaluation about participant's own somatic responses such as sweaty palms and chills [17] were included. The questionnaire asked participants to write their age and gender in the blanks on the sheet and describe their knowledge of the story and the artist in the recorded performance. The questionnaire also asked participants to describe their impressions of the performance. In addition, participants filled out information on their familiarity with Rakugo performances by (1) using media and (2) going to the theatre in their everyday lives.

2.1.4 Procedure

The participants were separately invited to the laboratory room where the experimenter explained the experiment. To lessen the possibility that each participant intentionally controlled his/her eyeblink response, the experimenter withheld the actual purpose from the participants. Instead, the experimenter told the participants that the experiment "aimed to examine where you look on the monitor by measuring and recording

the eye points while appreciating a Rakugo performance." After briefly explaining the eye-tracking device, a nine-point calibration was performed. The experimenter recorded the air temperature and humidity at the starting point and checked to ensure that the videos worked well. The experimenter played a video (a muted movie of fish swimming in a group), while measuring and recording the eyeblinks of each participant as an individual frequency and asynchrony baseline within each group. Each participant was then instructed how to play the movie and the experimenter left the room. Participants started to play the assigned video on their own, while the device was measured and recorded their eyeblinks. After finishing the video presentation, the experimenter re-entered the room and asked the participants to complete the questionnaire. The experimenter explained that the actual purpose of the experiment was to measure the timings and frequency of eyeblinks while watching the storytelling performance. All participants gave permission for their eye information to be used in the study and agreed to answer the questionnaire. In addition, the experimenter asked if they had noticed that this was a study on eyeblinks. Five participants answered that they had noticed the eyeblink data, of which three were omitted from the analysis due to incomplete data (see, Participants). The other two participants suspected that the device might be related to eyeblink measurement; however, their eyeblink data were included in the analysis because they stated that they did not change the timing of their eyeblinks intentionally.

2.1.5 Analysis

2.1.5.1 Distance-based analysis of blink (spike) trains: Asynchrony

Victor and Purpura [1] proposed methods to quantify the asynchrony of two particular spike trains (e.g., time series of intermittently firing neurons) focusing on the difference of spike timings. *D spike* and $D^{interval}$ equally evaluate the distances of two different blinking trains (Fig. 1). However, only *D spike* calculates the distance at each time point of the spikes. In contrast, $D^{interval}$ takes into account the intervals of spike-by-spike. While these methods have been developed with the aim of analyzing asynchrony in firing neuron spike trains, they can be used to quantify the degree of asynchrony of particular blink trains.

D^{spike} is sensitive to inter-spike intervals. In contrast, $D^{interval}$ is sensitive to tem-

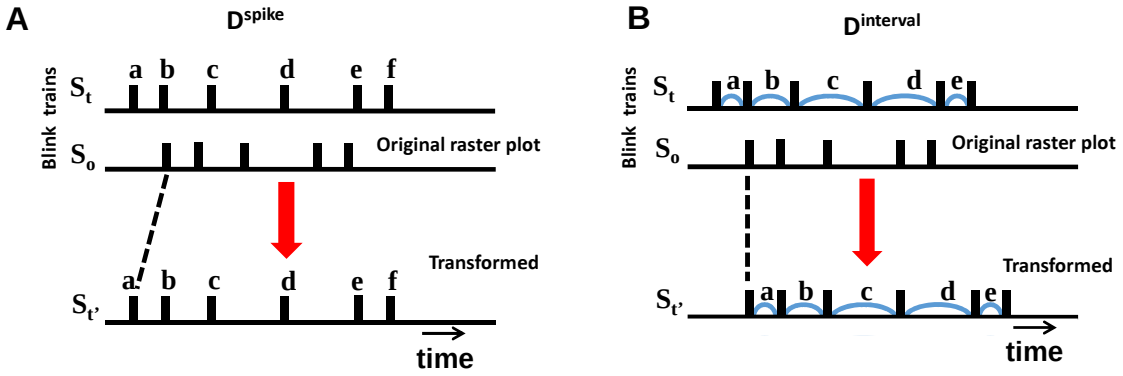

Figure 2.1: **Schematic illustrations of D^{spike} and $D^{intervals}$** (A) The distance between the two spike trains, S_t and S_o, is equal to seeking a path of the minimum cost, which transforms $S_o - S_{t'}$, with spike times (a, b, c, d, e, f) equal to S_t. (B) The distance between S_t and S_o is equal to seeking a path of the minimum cost, which transforms $S_o - S_{t'}$, with IBIs (a, b, c, d, e) equal to S_t. The authors originally created these two schematic illustrations based on Ref. [1].

poral spike patterns. Although a $D^{interval}$ value is constantly equal to or smaller than that of D^{spike}, there is no difference between the values of these indices if a particular temporal pattern is started at the same time. However, the value of $D^{interval}$ becomes smaller than that of D^{spike} when spike trains exhibit the same temporal pattern (motif) with a time delay in each time train [1]. Thus, the differences between these indices represent the degrees of pattern formation of IBIs. In other words, the difference in the value of $D^{interval}$ compared with that of D^{spike} suggests the ratio explained by the pattern similarity. If the viewing experience influences a situation model constructed through a viewing performance, a significant difference of pattern similarity will be found between experienced and non-experienced audiences.

In this study, the analysis unit was set to 250 [ms] because a blink usually occurs at an interval elapse of least 300 [ms] due to physiological limits [11]. That is, the whole video recording was divided into huge numbers of time windows (i.e., bins), each of which with a length of 250 [ms], and the distance was counted based on the number of bins. To evaluate asynchrony of each scene during the performance, time trains of 5 min of performance time each (i.e., 1200 units = 4(bins/s) × 60(s) × 5 (min.)) were used for calculation. As the total length was different with each video, the last 50 min. of video footage was accurately divided into 10 scenes (i.e., each scene containing 5 minutes of footage). The rest (i.e., the first 22 s in the video for frequent viewers and

220 s in the video for first-time viewers) was excluded from the time-series analysis.

All values of D^{spike} and $D^{interval}$ were calculated using a modified version of a program provided by Ref. [1]. The program was mainly developed in the Matlab and Visual C++ environment. All p-values were two sided and a p-value of .05 or less was assumed statistically significant. All statistical analyses were performed using EZR (Easy R, Saitama Medical Center, Jichi Medical University; [27]), which is a graphical interface for R (The R Foundation for Statistical Computing, Vienna, Austria, version 3.0.2).

2.1.5.2 Detecting the onset of laughter elicited in situ

To detect laughter, videos recorded in 30 frames per s were coded using ELAN 4.5.1 (Max Planck Institute for Psycholinguistics, Nijmegen), which has been developed for analyzing discourse processes and interactions among small-group members in face-to-face communication. The period of laughter was detected in the frame as the smallest unit (33.4 Hz) using only the sounds of the video. Each first frame was set as the onset of that laughter. A researcher trained in the methods of psychological study performed the coding procedure.

2.2 Results

2.2.1 Operational checks

2.2.1.1 Laboratory environment and time delay of stimuli presentation

No difference in the degree of laboratory humidity was found among the groups. Differences of time delays among the groups were not significant (range 501 ± 88.69 [ms]).

2.2.1.2 Audience knowledge about the performer and the story

None of the non-experienced participants knew either the performer or the story. On the other hand, approximately a half of the experienced participants knew the performer (the orthodox performance: 46.67 % and the modified performance: 33.33%) and the story (the orthodox performance: 66.67 % and the modified performance: 46.67 %). (2.1).

Table 2.1: Percentages of participants with knowledge of the performer and the story.

	Experienced participants	Non-experienced participants
Knowledge in advance of the performer		
Typical performance	46.67	0.00
Modified performance	33.33	0.00
Knowledge in advance of the story		
Typical performance	66.67	0.00
Modified performance	46.67	0.00

$n = 15$ for each group.

2.2.1.3 Reliabilities of scales

The α coefficients of the scales were .77 and .91 for humor and experience of transportive experience, respectively. The coefficients were high enough for the following analysis.

2.2.1.4 Baseline of asynchrony

To confirm that there was no difference in the total count of eyeblinks per time between groups, ANOVA was used for the IBI expressions of performer and viewing experience of the audience. The results showed no main effect and no interaction. Thus, the total rates or total numbers of eyeblinks were not different among the groups. This result was supported even if the participant's age, a factor that may have influenced the total numbers of eyeblinks, was taken into account. Under the baseline condition, only the main effect of audience viewing experience was significant ($F(1, 338) = 9.84$, $p < .01$). The experienced audience value of $D^{interval}$ was lower than that of the non-experienced audience (.62 vs. .70, $p < .05$ for orthodox video and .60 vs. .71, $p < .10$ for modified video, respectively). This fact may indicate that experienced audience members slightly tend to synchronize their eyeblinks even when they are watching a video unrelated to domain knowledge (silent movie of a group of fish). Owing to this result, in section 3.4.2, differences between the value of $D^{interval}$ for experienced and that for non-experienced audiences were accepted only when the effect size of this comparison exceeded that of the baseline, and statistical values were significant. The values of asynchrony under the baseline condition in each group were relatively lower than those during video screening. Because the stimulus used in the baseline condition contains only visual information, the timing of the allocation would converge.

On the other hand, storytelling performances included audio-visual stimulus requiring participants to integrate multimodal information.

2.2.2 Multiple regression analysis

The mean and standard deviation of IBIs followed logarithmic normal distribution according to the nature-of-time relevant variable. In the following analysis, logarithmic-transformed mean and standard deviations of IBIs were used. To examine the relationships between variables, zero-order correlations were calculated (Table 2.2). The coefficient of correlation between transportive experience and humor was very high ($r = .772$, $p < .001$). Knowledge of the performer positively correlated with transportive experience and humor. The SD of IBIs did not have a salient correlation with other variables.

Table 2.2: Zero-order correlation coefficients between variables used for multiple regression analysis.

	2	**3**	**4**	**5**	**6**
1. Transportation	0.772^{***}	0.071	$0.197^{\dagger}$	0.262^{*}	0.107
2. Humor	–	-0.008	-0.014	0.315^{**}	$0.191^{\dagger}$
3. Mean of IBIs		–	0.156	0.033	-0.028
4. SD of IBIs			–	0.085	0.105
5. Knowledge of the performer				–	0.703^{***}
6. Knowledge of the story					–

IBIs: inter-blink intervals, $N = 60$, $^{\dagger}p < .10$, $^{*}p < .05$, $^{**}p < .01$, $^{***}p < .001$.

In order to explore which variables predicted the experience of transportation, a multiple regression analysis was performed (Table 2.3). The results of multiple regression analysis demonstrated that humor strongly predicted the experience of transportation ($\beta = .772$, $p < .001$). SD of IBIs also regressed on the experience of transportation ($\beta = .208$, $p < .05$). The other variables such as age, gender, means of IBIs, and domain knowledge (the performer and the story, dummy variables) exhibited no significant effects. The zero-order correlations between the domain knowledge and transportive experience were weakened by taking the other variables into consideration. The coefficient of determination was considerably high ($R^2 = .64$).

Table 2.3: Zero-order correlation coefficients between variables used for multiple regression analysis.

	B	SE	**Standardized** β	t**-test**
Intercept	0.362	0.726		0.499
Humor	0.503	0.056	0.772	9.064^{***}
Mean of IBIs	0.047	0.101	0.038	0.462
SD of IBIs	0.432	0.171	0.208	$2.525\ *$
Knowledge of the performance	0.102	0.140	0.085	0.724
Knowledge of the story	−0.128	0.121	−0.121	−1.059

IBIs=inter-blink intervals $R = 0.806$, $R^2 = 0.649$ $^{*}p < .05$, $^{***}p < .01$.

2.2.3 Experience of transportation

To reveal the effect of the performer's expressions and audience viewing experience, the factor design was a two-way ANOVA performance (between the two levels; for frequent viewers and first-time viewers) × experience of audience (between the second level; experienced and non-experienced). The dependent variables analyzed included the score of humor scale and the score of the transportation scale. When humor and transportation scale scores were combined, the main effects and interaction between performance and experience of audience were not significant. For the transportation scale score, the effect of experience was marginally significant, indicating that the score of the experienced audiences was very slightly higher than that of the non-experienced ($F(1, 56) = 2.963$, $p < .10$, experienced 2.58 vs. non-experienced 2.37). In addition, the simple main effect (corrected Bonferroni's method) of the experienced audiences was marginally significant (.30, $se = .17$, $p < .10$, experienced 2.69 vs. non-experienced 2.39).

2.2.4 blink synchronization

2.2.4.1 Estimated similarity of IBI patterns

The difference between and D^{spike} indicates the similarity of the IBI patterns within two trains (Fig. 2.2A, B). As the results of the two-way ANOVA (viewing experience × video) data of 10 scenes showed, the main effect of the viewing experience was significant ($F(1, 2066) = 25.38$, $p < .0001$, Fig. 1D). Sub-effect tests revealed that the estimated similarity in eyeblinks of the experienced audience was higher than that

of the non-experienced audience in both performances ($p < .001$, 0.15 vs. 0.09 and $p < .05$, 0.14 vs. 0.11). In addition, the estimated similarity in eyeblinks during the orthodox video was higher than that of the modified video ($p < .01$, 0.12 vs. 0.10).

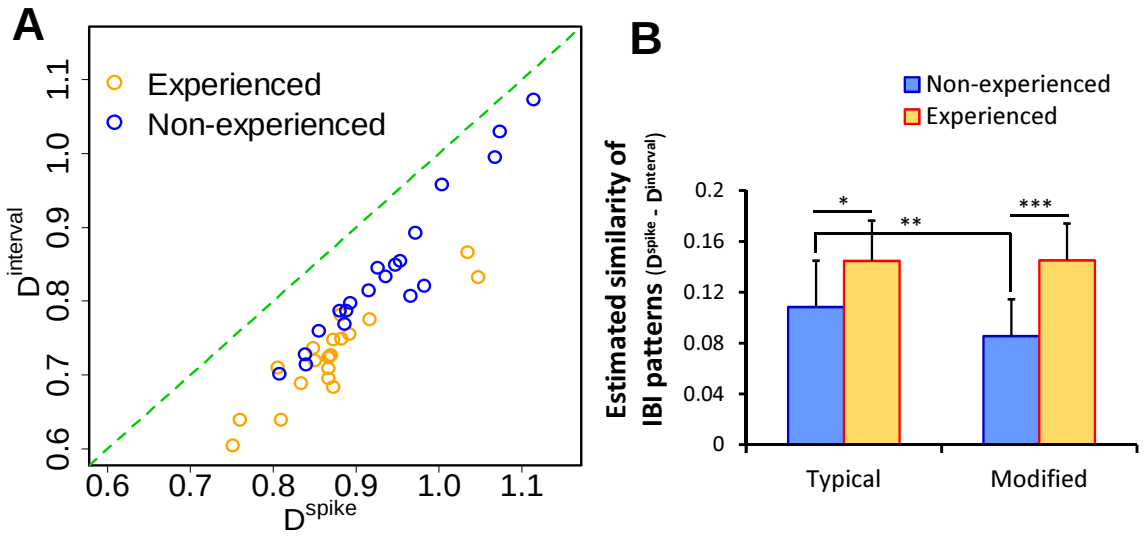

Figure 2.2: **estimated similarity of inter-blink interval (IBI) patterns.** (A) The scatter plot of $D^{interval}$ and D^{spike}. The coefficient of determination $R^2 = 0.87$. (B) Similarity of IBI patterns within each group estimated from the difference between $D^{interval}$ and D^{spike}. $^{*}p < 0.05$, $^{**}p < 0.01$, $^{***}p < 0.001$.

2.2.4.2 Temporal pattern of $D^{interval}$

In the first six scenes ($0 - 30$ min) of each video, the average $D^{interval}$ within a group of experienced participants was significantly higher than that of the non-experienced participants, except for 25 min. of the orthodox performance. All effect sizes of these comparisons exceeded those of the comparisons observed under the baseline condition. Regarding homogeneity of variances, the null hypothesis that the true ratio of variances is equal to 1 was rejected at $D^{interval}$ from 15 to 30 min of the orthodox video and during all $D^{interval}$ of the modified video (not shown in Fig.2.3). Overall, the index $D^{interval}$ of the participants who had viewing experience remained low while watching both the orthodox video (Fig.2.3A, orange line) and the modified video (Fig.2.3B, orange line). Non-experienced participants who watched the modified performance gradually reduced eyeblink asynchrony as the story developed (Fig.2.3B, blue line). On the other hand, even non-experienced participants had reduced asynchrony as of the first

few minutes to the end of the story while watching the orthodox video (Fig.2.3, blue line). The standard deviations for experienced participants also stayed relatively small while standard deviations for non-experienced participants decreased throughout the performance.

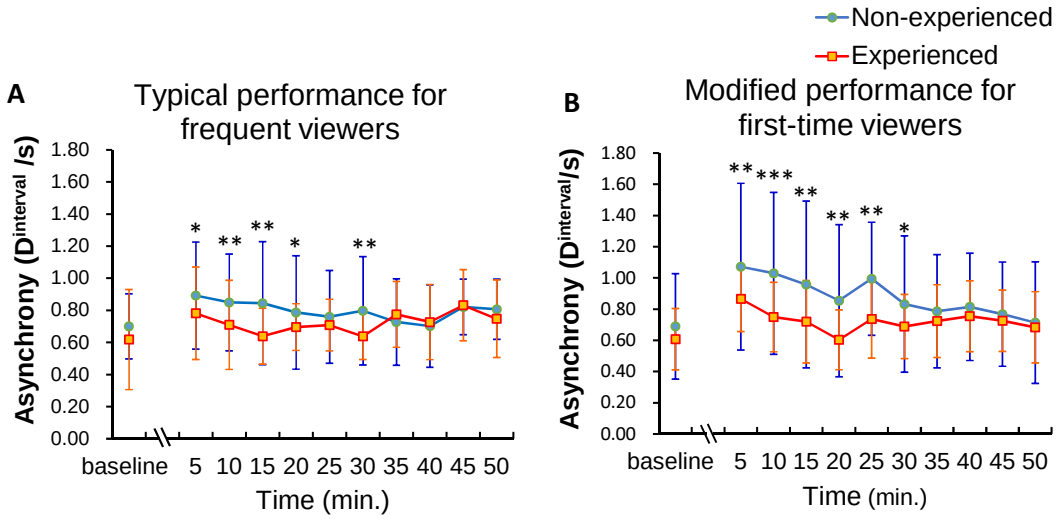

Figure 2.3: **Asynchrony of eyeblinks among participants at each scene (5 min) During appreciation of videotaped performance (A), which is typical for frequent viewers, and (B), which is modified for first-time viewers.** Mean $D^{interval}$ among all possible pairs within each group were calculated. Error bars shows the SD. Asterisks and obelisks indicate the p-values of t-tests assuming unequal variance, which were performed in each scene between experienced audience vs non-experienced audience. P-values corrected by the method of Bonferroni were used. $^{*}p < 0.05$, $^{**}p < 0.01$, $^{***}p < 0.001$.

2.2.4.3 Effect of laughter

In the case of the orthodox performance, the results of abovementioned ANOVA demonstrated relatively lower levels of $D^{interval}$ for even non-experienced participants as of the beginning of the performance. However, these effects for non-experienced participants were not observed in the modified performance, possibly because of the differences between audience responses in situ reflecting changes in the emotional expression of the performance. In order to reveal the possible influence of laughter on the difference in $D^{interval}$, the number of eyeblinks occurring at, before, and after the onset of laughter was compared. A three-way ANOVA was performed on the number of eyeblinks in each unit was normalized to a z-score across the performances (Fig.2.4).

The factor design of this ANOVA was video (between the two levels; orthodox and modified) × experience of audience (between the two levels; experienced and non-experienced) × timing (between the twelve levels; the time of 6 units before onset and 6 units after onsets of laughter). First, Mauchly's test was conducted to check sphericity. All of the test statistics were not significant. We then used type III sum of square repeated measures ANOVA assuming sphericity. The main effects of time were significant ($F(11, 3916) = 1.853$, $p < .05$) and none of the other main effects and interactions were significant. To identify the sub-effect, a two-way ANOVA for each video (orthodox and modified) was exerted. The results demonstrated that the main effect of timing was significant during the orthodox video ($F(11, 2420) = 2.21$, $p < .05$). We performed one sample t-test for the mean against the null hypothesis ($\mu = 0$) using a p-value collected by the Bonferroni's method. Only a time point $1.25 - -1.50$ [s] after the onset of laughter in the video was significantly higher than 0. All means at the other time points were not significant for rejecting the null hypothesis.

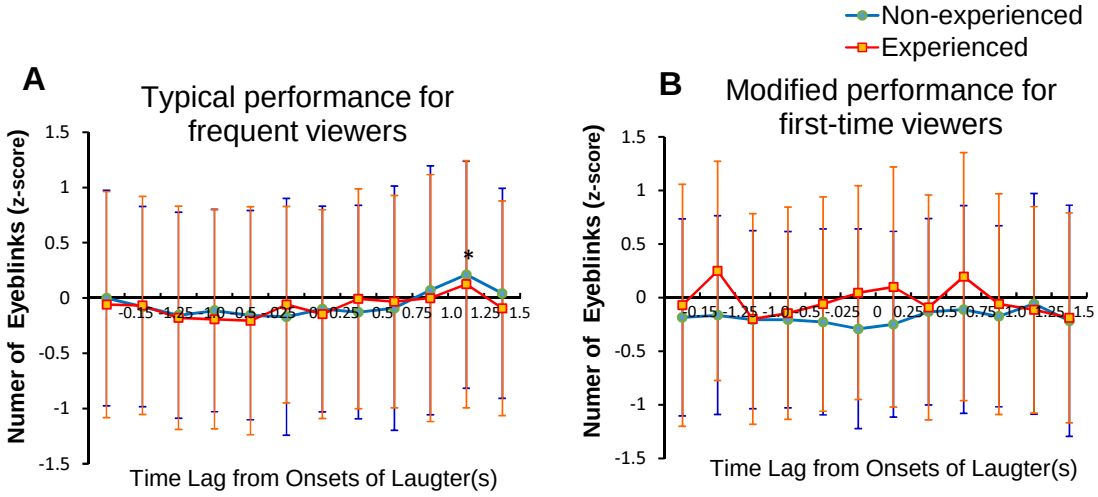

Figure 2.4: **z-scores of eyeblinks before and after onsets of laughter** Z-scores recorded in performance (A) Typical and (B) Modified. Error bars show the SD. An asterisk indicates a p-value of one sample t-test for the mean against the null hypothesis. P-values corrected by the method of Bonferroni were used. $^*p < 0.05$.

2.3 Discussion

2.3.1 Mechanisms of transportation

Participants' eyeblinks synchronized among the non-experienced audience at a level equivalent to that of the experienced participants through an appreciation of the performance (Fig. 2A). As enough information seemed to be presented in each performance, even non-experienced participants appeared to be able to construct a situation model using only a temporally accumulated knowledge of the story by comprehending the storyline and the personalities of the characters. On the other hand, the standard deviations of the experienced participants tended to be lower than those of the non-experienced participants. This result suggests that the audience's domain knowledge cultivated by viewing experience aids in the construct of similar situation models among the audience. The results of estimated similarity of the IBI pattern (Fig. 1C) also suggest that experienced audiences, compared to non-experienced audiences, respond in more reproducible ways within each group. Although not all experienced participants knew the story or the performer perfectly, the experience of the participants helped to synchronize their eyeblinks. Thus, results were obtained by application of knowledge regarding typical developing patterns of storylines in the field of Rakugo performance.

However, in this experiment, the situation model supported by domain knowledge did not explain an experience of transportation fully (Fig.2.3B). The results of the ANOVA concerning transportation showed that the main effect of audience experience was weak. The results of the multiple regression analysis indicated that humor and standard deviation of IBIs predicted a transportive experience. Other variables had no predictive effects. In Ref. [15] van Laer et al. reveals that age, gender, and knowledge gained by education, among other variables, affects the degree of a transportive experience, based on a review of several articles (e.g., [28] [29]). However, the apparent effects relating to the degree of viewing experience and other demographic variables seem to be peripheral. The standard deviation of IBIs suggests that an individual's allocation of attention varies more frequently as he or she is inclined to predict upcoming events [3]. It could be said that the eyeblink-rate variability is accompanied by emotional excitement. This emotionally motivated eyeblink-rate variability might be attributed to the expressiveness of a performance and corresponding humor in situ. Because the same story was performed by the same performer, the differences of asyn-

chrony must depend on the performance rather than the structure of the story. As described so far, the two mechanisms that we mentioned earlier seemed to be confirmed. It was suggested that the emotionally excited eyeblink-rate variability could be a good predictor of transportation.

The possibility of eyeblink occurrence increased at $1.25--1.50$ [s] after the onset of laughter. This result suggests that laughter by the surrounding audiences functions as a cue for further processing [30]. A time delay from the onset of laughter may be due to a time lapse between recognition and reinterpretation of a situation in the story. However, the effect was confirmed only during the orthodox performance. For non-experienced audiences, estimated pattern similarity (i.e., formation ratio of temporal patterns, "motif") was also higher for those who watched the orthodox video than those who watched the modified video, as shown in Fig.2.3B. These results suggest that even non-experienced audiences synchronize their eyeblinks, to some extent, when appreciating a performance acted in the orthodox way usually seen in theatres. The performance that amuses experienced audiences would seem to simultaneously exert this effect on non-experienced audiences.

Although the effect of the viewing experience was confirmed, it was weak. A non-experienced audience might devote significant cognitive resources to comprehending the contents of the story, leaving very little for other resources. In contrast, an experienced audience might be engaged in a transportive experience by sparing cognitive resources in order to appreciate the details of expression, especially for an orthodox performance. The experienced audience might sometimes pay attention to a particular nuance of expression by each artist rather than simply enjoy the contents of the performance per se. Actually, in the free description about their impressions of the performance, some experienced audience members answered that the performer appeared to inherit the traditional style of Rakugo compared to the other performers in his generation. A viewing experience does not always lead to transportation. An implicit selection of information and a resupply of emotionally excited attention lead to a precise prediction of the next plot twist and an engrossing experience. Overall, a transportive experience would actualize under a situation in which both active leading by performance and active anticipating by the audience occur. In this sense, a performer and audience share the responsibility to create transportive enjoyment in a vaudeville setting. A performer would act as the leader in providing his/her creative expressions and the

audience would play the role of actively anticipating the created world of the story.

2.3.2 Dynamic indices and future direction

The findings about the underlying mechanisms in real-time processing are significant in the research field of transportive experience that has focused on the traits of the receiver (see Ref. [15]). In particular, the predictive power of eyeblink-rate variability during viewing performance implies that people experience transportation through active coordination of specific external audio-visual information. Both blink synchronization and eyeblink-rate variability could be useful measurements for researchers to infer the inner experience of audience members by observing unintentional behaviors objectively. The results of this study also suggest that emotional excitement motivates more attentional cognitive resources onto the actor's expressions and the structure of the story. In this study, the positive emotion (i.e., humor) is strongly related to the transportive experience because the performance is oriented to create a sense of enjoyment or exhilaration in the audience in a vaudeville setting. However, it is not surprising if the feelings of thrill or suspense predict a transportive experience at the cinema. Future research is necessary to examine the relationships between excitement of other kinds of emotion and transportive experiences.

A possibility exists that transportation is weakened compared with that experienced through live performance because a videotaped performance cannot preserve the atmosphere in situ. Further study is necessary to clarify whether or not emotionally excited eyeblink-rate variability more strongly facilitates the transportive experience in real vaudeville settings. Although the humor experience was evaluated retrospectively owing to operational limitations in this study, future research will reveal the time-sequential relationships between transportation, emotional excitement, and eyeblink-rate variability by measuring ongoing physiological indices such as skin conductance, heart rate, and aspiration rhythm.

In the first experiment, blinks among participants synchronized frequently and strongly under the condition where the participants viewed the expert story-telling performance, compared to that where participants viewed the novice performance. The results suggest that blink synchronization occurred in response to the appeal power of the expert performance because other most of possible variables were controlled by using the same story and by assigning the participants to be approximately equaled

regarding their viewing experience. In this setting, it seemed that the appeal power of performance changed the participants' timing of attention allocation. Consequently, participants become to blink in closer timing when to view. Blink synchronizations induced by common inputs appears that occurrences of temporally increase of blinking density rather than the precise co-occurrence of blinks. Previous studies in blink bursts are also supported the blink synchronization as the covarying of blink rates [31].

In this chapter, blink synchronization was defined as the average lower editing cost between a pair of time series of blinking timing as a point process. The results demonstrated that the degree of blink synchronizations was higher for frequent viewers than first-time viewers both in two recorded performances. The results suggest that knowledge about the performance and the performer helps to make segmentations of the visual information in accordance with the professional performance, leading the resemble blinking patterns. The results also demonstrated that the larger variance of the IBI related to the more transportive experience into the narrative world. Common inputs that is able to establish blink synchronization may elicit cognitive entrainment among audience members in theatre.

Chapter 3

Inter-Spectator Interactions facilitate blink synchronization

If blink synchronization occurred only due to the common inputs of the story-telling artist, then interactions would neither have attractive nor repulsive effects among audience members. In this case, the results would demonstrate no differences between these two groups, i.e., audience in situ vs. participants in the individual experimental setting as shown in Chapter 2. On the other hand, if interactions among audience members were also due to blink synchronization within the audience, systematic differences would be found. Moreover, if the collective nature of audience members was cooperative, interactions would have an attractive effect. If the collective nature was competitive, interactions would be repulsive. Therefore, in the former case, the results would show that eyeblinks would synchronize more in situ than in the individual experimental setting. In contrast, for the latter case, the results would occur in the opposite way. Regarding the cooperative nature, it could be hypothesized that it occurs by facilitating cognitive entrainment, which decreases each audience members' cognitive load. This hypothesis would be supported if the attractive effect were stronger for first-time viewers than for frequent viewers. However, if this cooperative nature was caused by mere somatic entrainment among audience members regardless of domain knowledge, there would be no difference found in blink synchronization based on audience members' viewing experience. In this chapter, I examine the influence of surrounding audience members on blink synchronization.

3.1 Method

3.1.1 Participants

Participants in the experimental condition (audience members) included 31 frequent viewers (mean age = 44.37, $SD = 13.57$) and 24 first-time viewers (mean age =28.06, $SD = 13.91$) for two separate performances, respectively. We defined frequent viewers in this study as the participants who had viewed Rakugo (Japanese traditional storytelling performance) more than 10 times regardless of type. The reason why we adopted this criterion is that the mean number of viewing times in the daily lives of most Japanese people is usually three or four. This means that a participant who meets our criteria as a frequent viewer would seek opportunities to view the Rakugo performance more than the average Japanese person would. Seven (five male and two female) frequent viewers and seven (five male and two female) first-time viewers were selected from each audience group as the targets whose eyeblink responses would be observed. This is due to the limitation of the observation method: the experimenter could only detect the eyeblink responses of these participants by the recorded faces. As all of the observed targets sat facing forward instead of facing the audience, the targets were limited to obtaining visual information only from the performer. In other words, the participants were not able to look at each other's faces or see each other's eyeblinks. The participants in the control condition (see Chapter 2) included 24 males and 36 females. Half of the participants were frequent viewers and the others were first-time viewers. The experimenter used the same criteria based on the participants' viewing experience to divide them into frequent viewers and first-time viewers. All participants provided their written informed consent to participate in this study. This experiment was approved by Life Science Research Ethics and Safety, the Ethics Committee of the University of Tokyo.

3.1.2 The storytelling artist and performed story

Rakugo is a traditional Japanese art of storytelling in which one artist plays many characters by changing face directions and sitting postures. Moreover, since the artist acts without lighting effects, visual information of the performer stays the same even when the scene changes. Therefore, the changes of characters and of scenes are interpreted

by acting conventions among the performer and audience members. In order to understand the story, the audience members themselves must work to make non-obvious segmentations on the continuous performance. In order to investigate the particular impact of story-telling performances, the authors used Rakugo performances, on which only minimal visual and sound effects are added, for this experiment. Because each artist is classified into three grades in accordance with their acting abilities, the author was able to validate the quality of the artist in this study. The artist of the live Rakugo performance was Bungiku Kokontei (34-year-old with 10 years' worth of experience as a performer) who is one of the highest-graded artists. The performed story was one of the classic Rakugo repertories, "Nibansenji," which literally means the second brew of tea or decoction. The performance for frequent viewers was conducted in the style of traditional vaudeville storytelling performances in everyday theatre (Orthodox version). The performance for first-time viewers was modified to allow the first-time viewers to better comprehend the content of the story (Modified version). The total time of the performances were 3022 seconds (s; 50 minutes (min.) 22 s) and 3220 s (53 min. 40 s), respectively. For the first-time viewers, the artist took a few minutes to explain the traditional way of viewing this type of storytelling performance. In the experiment settings, the experimenter used the video clips of the live performances.

3.1.3 Data collection

To detect the eyeblink responses, the analyzer utilized ELAN 4.5.1 (Max Planck Institute for Psycholinguistics, Nijmegen), which was developed for discourse analysis. When using this software, an analyzer can easily record many types of annotations on utterances and gestures (e.g., the onsets or offsets of a particular gesture). The onset of an eyeblink was defined as the frame prior to the frame in which the pupils were covered by the eyelids after a target audience member started blinking. An analyzer who had two years' worth of Rakugo-performing experience coded the eyeblink responses using the video recording of the audience (33.4 Hz) that was muted to eliminate the possibility of being influenced by the recorded voice of the performer. An analyzer also reduced the playing speed by approximately 60% of the original video, thus preventing the analyzer from missing the target's eyeblinks due to his own eyeblinks. If the motion of eyelids did not cover the whole eye surface area, it was coded as a muscle artifact and was not used in the analysis. To confirm coding reliability, the first author sepa-

rately coded one of the targets using the same procedure. As both coders concurrently identified more than 95% of the eyeblinks, the data coded by the analyzer were used for the consequent analysis.

3.1.4 Procedure

Participants were invited to enter the vaudeville setting recreated in the laboratory room. Six seats (three seats by two lines) were reserved for the first six participants of the experiment. The other seats were free seating. For first-time viewers, the experimenter explained the procedure of Rakugo performances (e.g., a storytelling performer changes his voice and turns his face to play many characters by himself). Then, the artist went to the center of the stage while a classic Japanese theme song played on the speakers. The artist sat down on the square cushion to start the performance. After the performance, the artist left the room. The experimenter and assistants distributed questionnaires to the participants in order to obtain their demographic variables and assess their domain knowledge regarding this kind of performance.

3.1.5 Distance-based analysis of blink (spike) trains: Asynchrony

Victor and Purpura [1] proposed a method to quantify the asynchrony of two particular spike trains (e.g., the time series of intermittently firing neurons) focusing on the difference of spike timings, $D^{interval}$. This method does not assume a Euclidean notion of distance. Rather, it adopts a metric space to define the distance, and then the method can be applied to the time trains of eyeblink occurrence [32]. In this study, $D^{interval}$ was used to evaluate the distances of two different blinking trains. The distance between the two spike trains, S_a and S_b, is equal to seeking a path of the minimum cost, which transforms S_a-S_b, with IBIs (a, b, c, d, e) equal to S'_b. If the original pattern of Sb is more similar to S_a, the cost of transforming is lower. Hence, $D^{interval}$ quantifies the asynchrony between two particular time trains. In this study, the analysis unit was set to 250 milliseconds [ms] to maintain a format of results similar to that of the control condition results, reported in Chapter 2. In other words, the entire video recording was divided into many time windows of 250 [ms] width (i.e., bins). To evaluate the asynchrony of each scene during the performance, time trains of

5 min. of performance time each (i.e., 1200 bins = 4 bins/s × 60 [s] × 5 [min.]) were used for calculations as in the control condition. Welch's tests of the mean $D^{interval}$ in situ vs. the mean $D^{interval}$ in the experiment were performed for each scene using Bonferroni-adjusted p-values.

3.2 Results

In Chapter 2, I reported that the eyeblinks of frequent viewers synchronized than that of first-time viewers during the first 30 [min.] of the performance in both videos (Orthodox version and Modified version). This effect of viewing experience on blink synchronization was especially stronger in the Modified version (Fig.2.2B). In contrast, the results observed in the live performances in this study demonstrated that both the $D^{interval}$s of frequent viewers and that of the first-time viewers were much lower than those of each control condition (black lines in Fig.2.2A and Fig.2.2B), indicating that eyeblinks synchronized in situ rather than in the individual control condition, regardless of the version of performances. For frequent viewers, there was no difference in the asynchrony of eyeblinks at the starting point of the story despite the format of the Orthodox version of the performance (Fig.2.2A, orange line and black line). However, the asynchrony ($D^{interval}$s) of the audience members' eyeblinks in situ decreased as the story progressed (from the fifth scene to the tenth scene, respectively: $t(37.10) = 5.77$, $p < .001$; $t(37.10) = 5.80$, $p < .001$; $t(61.19) = 9.45$, $p < .001$; $t(70.70) = 9.26$, $p < .001$; $t(43.02) = 8.75$, $p < .001$; $t(71.43) = 9.84$, $p < .001$). As a result, asynchrony was lowest during the last 5 min of the performance, including the final remark (punch line). In contrast, in the performance of the Modified version (Fig.2.2B, blue line and black line), throughout the whole story, there were major gaps between the asynchrony ($D^{interval}$s) gained from in situ and that acquired from the experiment for first-time viewers (from the first scene to the tenth scene, respectively: $t(118.81) = 8.61$, $p < .001$; $t(118.81) = 10.06$, $p < .001$; $t(120.32) = 8.97$, $p < .001$; $t(98.26) = 6.50$, $p < .001$; $t(70.62) = 11.91$, $p < .001$; $t(99.82) = 8.42$, $p < .001$; $t(72.98) = 7.08$, $p < .001$; $t(57.20) = 6.97$, $p < .001$; $t(57.43) = 6.93$, $p < .001$; $t(100.44) = 7.79$). The asynchrony of the first-time viewers' eyeblinks in situ was lower (Fig.2.2A, black line) even when compared to that of the eyeblinks of frequent viewers (Fig.2.2B, black line).

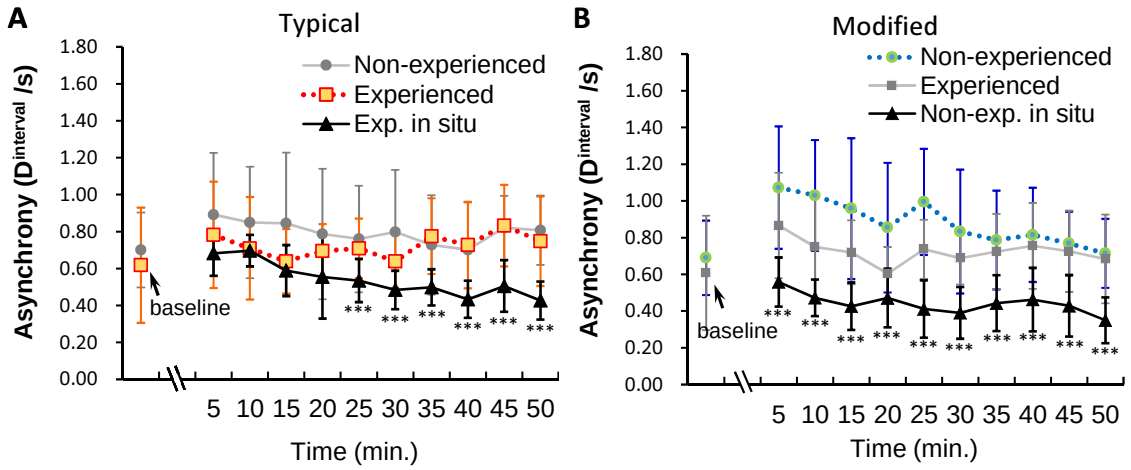

Figure 3.1: **Asynchrony of eyeblinks among participants at each scene during observation of the performance.** (A) Typical live (black line) and videotaped (orange dashed line) performances for frequent viewers, and (B) modified live (black line) and videotaped (blue dashed line) performances for first-time viewers. Both dashed lines and gray lines show data reported in the above section. Error bars show the sd. Asterisks indicate the p-values of Welch's tests, which were performed for each scene between the mean $D^{interval}$ in situ vs. the mean $D^{interval}$ in the experiment. Bonferroni-adjusted p-values were used. $^{***}p < .001$.

3.3 Discussion

3.3.1 Comparison between frequent viewers and first-time viewers

The purpose of the current study is to explore the effect of interactions among audience members on the cognitive aspect of entrainment in live performances. To assess the effect of interactions, the blink synchronization of audience members during live performances was compared to that of audience members in individual experiments. The results demonstrated that interactions among audience members facilitate blink synchronization. Although this attractive effect was found in both the Orthodox version for frequent viewers and the Modified version for first-time viewers, the estimated effect of interactions for first-time viewers was stronger than that of frequent viewers. First-time viewers would have to spare cognitive resources to comprehend a story. Hence, the cognitive load would be relatively higher for first-time viewers than frequent viewers. Previous research [33], [34] reported that as the cognitive load increased,

eyeblink rate increased. In this study, however, first-time viewers synchronized more their eyeblinks (i.e., showed lower asynchrony, $D^{interval}$, as compared to the experienced viewers). Occurrence timings of eyeblinks were found to be related to change in attentional state regardless of stimulus modality [35]. If one audience member can adopt clues of attentional processing from other audience members in a collective situation, even first-time viewers would lead cognitive entrainment at a smaller cognitive cost. It is suggested that first-time viewers enjoy the story by unintentionally utilizing other audience members' responses as clues for cognitive processing.

On the other hand, frequent viewers appeared to be relatively less influenced by the temporal responses of other audience members, since they internalized viewpoints of this domain based on their many experiences. The study in Chapter 2 reported that frequent viewers synchronized their eyeblinks by watching the same story-telling performance. Thus, frequent viewers seemed to enjoy the story based on individual cognitive processing and using their own domain knowledge.

Because all target audience members faced forward in their audience seats, they seemed to be influenced mainly by the laughter of other audience members instead of by visual information. A theory of humor [30] has suggested that further elaboration increases the experience of subjective humor. Laughter could be one of the clues indicating the occurrence of elaboration [30].

3.3.2 Advantages of the current study and future directions

This study analyzed blink synchronization in order to shed light on the cognitive entrainment that emerges because of interpersonal communications. This approach could provide a new perspective from which the dynamics of collective human behaviors in a temporally shared field might be examined. Audience members appeared to attract each other, leading to a mutual entrainment [36]. Eyeblink synchronization was also observed when individuals were watching the same storytelling performance separately [3], during which a forced entrainment [36] between the performer and each audience member would occur. In the actual theatre, these two entrainments would occur in complex ways. From the viewpoint of a complex system, blink synchronization is hypothesized to be a synchronization of multiple agents' periodic behaviors induced by the common inputs [14]. This performer-audience system includes both top-down inputs and bottom-up emergent processes [37]. Attractive effects of interactions among

audience members suggest that partly depending on other members who have received the same inputs could possibly be a mechanism of self-adaption [38] based on visual cues that are used in collective viewing situations. From this perspective, becoming an expert narrative artist is a process that involves acquiring adaptive control strategies to be used in uncertain situations where unexpected patterns of audience members' response usually occur.

However, in the current study, the interactions among audience members were estimated as the total mass. Thus, the results only roughly illustrate a sketch of the time developments of cognitive entrainment. In future research, it would be necessary to develop a model of an entrainment system between a performer and the spectators. Somatic entrainment and cognitive entrainment within an audience are still not well understood. Does somatic entrainment lead to cognitive entrainment, does cognitive entrainment lead to somatic entrainment, or is it mutual? This is a key question, as situations in which a speaker performs in front of spectators are ubiquitous in human cultures. The elaborated model must provide universal findings and strategies that are applicable to other kinds of oral performance, such as speeches, presentations, lectures, and so on.

3.4 Conclusion

Whereas the entrainment of movements and aspirations among audience members has been known as a basis of collective excitement in the theatre, the role of the entrainment of cognitive processes among audience members is still unclear. In this chapter, temporal patterns of the audience members' attention were observed using eyeblink responses. To determine the effect of interactions among audience members on cognitive entrainment, as well as its direction (attractive or repulsive), the blink synchronization of the following two groups were compared. The results of this study demonstrated that the mean values of a measure of asynchrony (i.e., $D^{interval}$) were much lower for the experimental condition than for the control condition. Frequent viewers had a moderate attractive effect that increased as the story progressed, while a strong attractive effect was observed throughout the story for first-time viewers. The attractive effect of interactions among a group of spectators was discussed from the viewpoint of cognitive and somatic entrainment in live performances.

Chapter 4

A model of Human Spontaneous Blinking

4.1 Introduction

Although numerous experimental studies on human spontaneous blinking have been developed [32], [39], [40], little theoretical research using mathematical models has been carried out. The one-dimensional stochastic diffusion (OSD) model has been proposed as a mathematical model of spontaneous blinking [41]. This model assumes a blink generator in which electrical potential varies depending on the external inputs of corneal stimulation such as dryness, dust, or muscle fatigue. The electrical potential varies as Brownian motion process, resulting in a blink when the potential reaches a threshold. The potential exponentially decays to a constant value when the blink generator receives no inputs. Thus, intervals between spontaneous blinks are formulated as a first-passage-time to a constant threshold. According to [41], burst patterns in blinking can be explained by assuming that the threshold was shifted lower when the participants were drowsy.

Human blinking rates, however, vary in a few tens of seconds while watching an audio-visual stimulus [42]. A realistic model should account for this variation. In addition to such temporal characteristics, changes in blinking rates often provide less common distributions of inter-blink intervals (IBIs) in cognitive tasks [31], [43]. Thus, an adequate model should reproduce the diverse distributions of spontaneous blinking. The OSD model cannot reproduce distributions of IBIs because of its stochastic nature

and constant threshold.

In this paper, we propose a leaky integrate-and-fire (LIF) model with a variable threshold to represent the fluctuation of internal states of human blinks. First, we examine the reproducibility of the distributions of IBIs by the OSD model, however, the OSD cannot reproduce experimental results. Then, we show that the proposed LIF model reproduces a variety of distributions such as the positively skewed, normal, peak-less, and bimodal distributions of IBIs. Finally, we explore the parameters that reproduce the distributions of IBI reported in a classical experimental study.

4.2 Model of Human Spontaneous Blinks

4.2.1 One-dimensional stochastic diffusion model

In this model, changes in the potential X of the blink generator are governed by the following equation:

$$dX(t) = \left(-\frac{X(t)}{\beta} + \mu\right) dt + \phi dW(t), \tag{4.1}$$

with an initial condition $X(0) = X_0$.

In Eq. (4.1), W is a Wiener process that is characterized by spontaneous decay β (> 0), average input μ ($-\infty < \mu < \infty$), and a noise term of ϕ (> 0) for a random process. This stochastic differential equation is formally equivalent to the Ornstein-Uhlenbeck process. The interval between one blink and the next (IBI) can be expressed as a first-passage-time density function, which is defined by the time duration between the initial potential X_0 and the time to pass the threshold potential.

The OSD model is based on the Ornstein-Uhlenbeck process and therefore the potential X obeys the mean reversion law [41]. If we took $P(\omega|\alpha, t)$ as the probability that a stochastic variable α is given when $t = 0$ whereby we gain ω at time t, in this model, $P(-\infty|X_0, t) = 0$. According to Hoshino [41], this mathematical assumption represents the physiological nature of a blinking generator that reliably repeats to active blinking within a finite time period without assuming a reflecting boundary.

The results of numerical simulations demonstrated that the OSD model can reproduce the positively skewed distribution of experimentally observed IBI [41]. However, this model does not reproduce the other previously reported distributions of IBI.

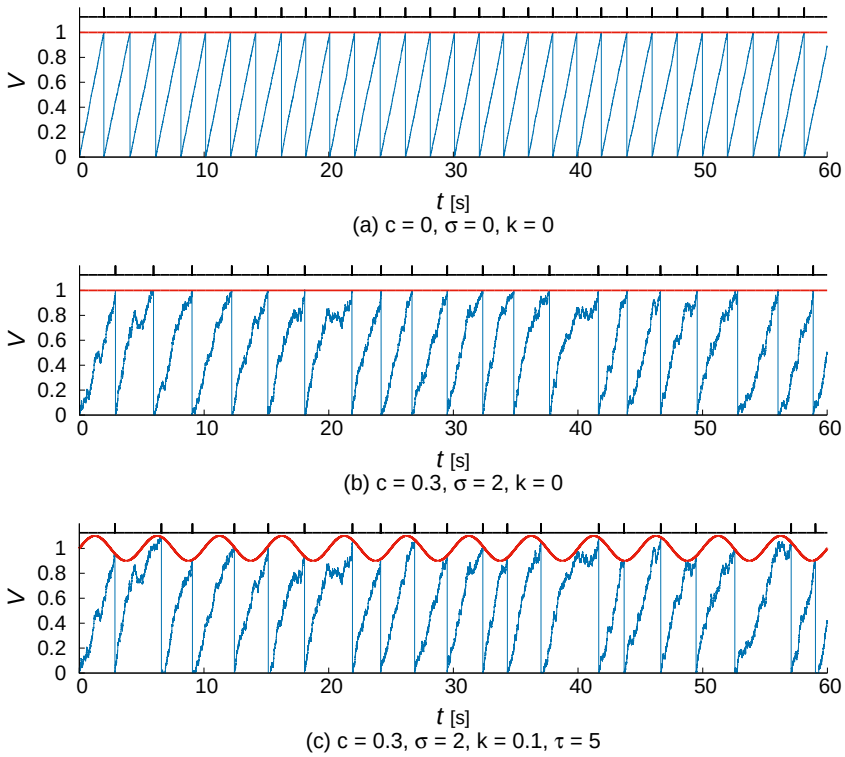

Figure 4.1: **Results by the LIF model with (a), (b) a constant and (c) a variable threshold.** The V increases with integrating the binomial input I. The parameter c is the decay term and the parameter σ is the standard deviation of noise ξ. The baseline of the threshold function $a = 1$. (a) There are no decay and no noise, i.e., $c = 0$ and $\sigma = 0$. (b) There is no noise, i.e., $\sigma = 0$. (c) The threshold is time-varying with the amplitude k and the period τ where the decay and the noise exist.

4.2.2 Leaky integrate-and-fire model with a variable threshold

Although the primary physiological function of blinking is to prevent dryness of eye-surfaces, cognitive functions of human blinks have also been reported [32], [18]. Human blinks in accordance with semantic segmentations of audio-visual information. For example, people tend to blink after looking at punctuation marks in reading tasks [18] and immediately after listening to the punch line of jokes while viewing a storytelling performance [32]. Neurological research indicated that spontaneous blinks contribute to disengaging attention from audio-visual stimuli [44]. Cognitive load is integrated while audio-visual information is continuously accumulated. When people blink, however, the cognitive load is reset by attentional disengagement where a part of audio-visual information is transmitted to the next processing stage. These facts indicate that we can model the biophysical changes in an internal value of a blink generator which is driven by cognitive load as well as by physiological inputs such as dryness and fatigue of muscle.

As one of the possible models, we used a leaky integrate-and-fire model with a variable threshold to represent such a blink-and-reset mechanism. The leaky integrate-and-fire models have been used as models of changes in membrane potential of a single neuron [45]. Human blinking is a macroscopic phenomenon that involves several brain areas. However, as long as we could assume that integrate-and-reset mechanism as a plausible postulation, the leaky integrate-and-fire model is suitable for human blinking as well.

As a possible mechanism for blinking intervals providing a variety of distributions, we assumed that the changes in blink rates are regulated by internal states that could vary in accordance with external stimuli. To construct the model, we assume a simply formulated situation where a background oscillation exists as a regulator of frequent human blinking. Such oscillation would emerge spontaneously as a result of physiological rhythms in addition to the rhythm induced by the external stimuli during an experimental task that requires visual attentions. In this study, we consider a leaky integrate-and-fire model with a variable threshold [46].

The potential V of blinking generator is governed by

$$\frac{dV}{dt} = -cV + I + \xi, \tag{4.2}$$

where c is a constant decay term and I is an external input with intensity b. The last term represents the Gaussian noise $\xi \sim N(0, \sigma^2)$ derived from the random fluctuation of external stimuli. The noise $\xi = 0$ when $\sigma = 0$.

One way to extract a particular rhythmic process in a physiological system is to set a variable threshold function [47]. Then, we introduced the following threshold function $\theta(t)$ determined by

$$\theta(t) = a + k \sin \frac{2\pi t}{\tau}, \tag{4.3}$$

where a is the baseline constant, k is the amplitude coefficient, and τ is the period. When V reaches the threshold, it immediately elicits a blink.

Figure 4.1(a) and (b) shows the typical pattern when $a = 1$ and $k = 0$, i.e. $\theta(t) = 1$. In a simple case of a perfect integrator without decay and noise, i.e. $c = 0$ and $\sigma = 0$, V demonstrates a monotone increasing with accumulating non-negative external inputs I (Fig. 4.1(a)). Even when the threshold is constant, V, in the integrate-and-fire model, behaves in a complex way due to the decay term c and the noise $\sigma = 0$, resulting in the creation of irregular IBIs (Fig. 4.1(b)). The parameter k determines the amplitude of the threshold function $\theta(t)$. Owing to the nonlinearity of the varying threshold function $\theta(t)$, IBIs can show rather complex patterns even if the external input I is constant.

Previous researches have revealed the effect in a modulation of the current in LIF models of a neuron numerically and analytically [45], [48], [49]. A modulation of the current can be mathematically transformed to the variations of threshold. Therefore, the LIF model with a variable threshold would provide results that correspond to the previous research on a neuron. However, the LIF model would also be useful to understand statistical behavior of the human blinking if the LIF model fit the data from physiological experiments.

4.3 Numerical Simulation and Analysis

4.3.1 Parameters

To the best of the authors' knowledge, no mathematical proof provides that first-passage-time density functions of the Ornstein-Uhlenbeck process always exhibits positively skewed distributions. Thus, the ODS model [41] may reproduce a variety of distributions when specific parameters are set. Hence, we re-examined the distribu-

tions simulated by the OSD model. In this replication, threshold potential was set to 1.0 and the parameters of the Ornstein-Uhlenbeck process were set as shown in Table 4.1 to cover the typical ranges of decay β and input μ that elicit blinking at realistic intervals. In the numerical experiments, the parameters β, μ, and ϕ are increased by the values denoted in the third column of Table 4.1.

Table 4.1: Parameters used in the OSD model.

	range	an increment
β	[0.01, 10.0]	0.01
μ	[0.1, 10.0]	0.1
ϕ	[0.5, 1.0]	0.05

In all simulations, the time step was set to $dt = 0.001$ s. The total time for observation was 50 min ($= 3,000$ s) to gain enough occurrences of IBI to estimate the distribution of human spontaneous blinking [50].

On the other hand, in the simulations of the proposed model, parameters were set as follows: the intensity of the external input I of which intervals obey a binomial distribution was set to $b = 1$. To explore a relatively wide range of intensities for the inputs, a constant threshold baseline $a = 1$ was set. When we assume the simple case with $c = 0$ and $\sigma = 0$, it is necessary to accumulate non-negative inputs $1,000$ times because $b \times dt = 0.001$. Considering the binomial distribution of I, $2,000$ steps were needed on average to reach the threshold baseline. In other words, the variable V reaches the threshold in an average of 2 s. For instance, in case that $k = 0.20$, this corresponds to a maximum deviation $1/5$ from the threshold baseline when $a = 1$. In case that $k = 0.0$, however, the threshold is a constant $\theta(t) = a$ because

$$k \sin \frac{2\pi t}{\tau} = 0.$$

The period τ corresponds to the frequency of the threshold function $\theta(t)$. For example, the frequency of the threshold is 0.1 Hz for $\tau = 10$ s and 10.0 Hz for $\tau = 0.1$ s. Figure 4.1(c) shows the typical pattern when $a = 1$, $k = 1/10$, and $\tau = 5$ s, i.e.

$$\theta(t) = 1 + \frac{1}{10} \sin \frac{2\pi t}{5}.$$

4.3.2 Evaluation of Distribution

Based on observation of human blinking behaviours, Ponder and Kennedy [4] reported four types of distributions of IBI. Although this study is classical, we focused on this study because it had reported all of known distributions. Moreover, the distributions were obtained from sufficient number of participants with using a certain procedure. Variations of distributions were consistent with that obtained in the following experimental studies [51], [40]. Thus, Ponder & Kennedy's [4] four types of distributions of IBI are very informative even in recent years. According to Ref. [4], the results show that most common distribution was positively skewed (62.0%, 31/50 people). The authors also observed peak-less distributions (22.0%, 11/50), bimodal distributions (12.0%, 6/50), and normal distributions (4.0%, 2/50).

We evaluated the peaks of simulated distributions of IBIs using kernel estimation of probability density. The kernel density function $\hat{f}_h(x)$ was estimated as

$$\hat{f}_h(x) = \frac{1}{nh} \sum_{i=1}^{n} K(u).$$

We used a Gaussian kernel function, which is described as

$$K(u) = \frac{1}{\sqrt{2\pi}} e^{-u^2/2},$$

where

$$u = \frac{x - x_i}{h}.$$

In this equation, x_i was the ith observed value and h was the bandwidth, n was the total number of x_i. For kernel density estimations, we used the C++ library [52] in which the optimal bandwidths h were calculated as the integral over the square of the curvature using the trapezoidal rule.

We then estimated the number of peaks in the simulated distributions by applying the peak-finding algorithm [53]. In order to detect peak(s), this algorithm differentiates the estimated probability density and finds the locations where the signs change from positive to negative. Each peak is determined relatively rather than absolutely because the probability density could be high depending on the bandwidth. Therefore, a peak was defined as the point that fulfills the following two conditions that the peak point

exceeds 0.1, and exceeds one quarter of the difference between the maximum value and the minimum values. If any probability density was incomputable due to low occurrence of blinking, the peak-finding algorithm was not applied to those specific results.

We evaluated the kernel-estimated distribution in the range of 0–20 s, which is the usual IBI range. We calculated the median of the results of the simulations for comparison with the means of experimental data, because the shapes of the distributions were diverse. For unimodal distributions, we used these median values to detect the skewness. If the time location of the peak was lower than the centre of the estimated range, we regarded the distribution as the positively skewed.

For bimodal distributions, we evaluated the time locations of two simulated peaks. We permitted differences within ± 0.025 s for each reported peak. For instance, if the time locations in the experimental data were 0.5 s and 5.5 s, we assumed that these peaks were reproduced when the first simulated peak was located between 0.475–0.525 s and the second simulated peak was located between 5.475–5.525 s. The width of each histogram bin in Ref. [4] was 0.5 s, and therefore the range was narrow enough to capture the simulated peaks.

4.4 Results

4.4.1 Distributions of IBI simulated by OSD model

Our simulations resulted in $901,000$ solutions for the OSD model. Then, 70.53% ($635,488/901,000$) of the solutions had a peak, while the remainder (29.46%) had no peak defined by the peakfinder algorithm; bimodal and other multimodal distributions were not detected. One third (30.84%, $195,985/635,488$) of distributions with a peak were positively skewed although the time location of the peak depended on the parameters. Otherwise (69.15%, $439,503/635,488$), the simulated distributions approximated normal distributions. Regarding the distributions without peaks, the probability density was approximately constant within the range of 0–20 s, which is chosen for the simulation. We considered that these results demonstrated peak-less distributions at least in this range. Thus, the one-dimensional stochastic diffusion model reproduced only positively skewed, normal and widespread peak-less distributions of IBIs.

4.4.2 Proposed model

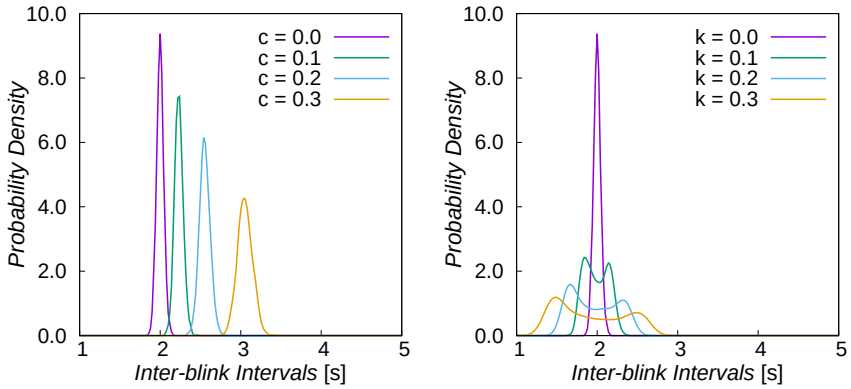

Figure 4.2: **Results obtained by the LIF model with a variable threshold.** Probability density functions change in accordance with decay term c or amplitude of threshold function k. (a) The symmetric shapes of distributions are maintained even when the decay term c becomes larger. (b) The tails of the distributions expand when the amplitude k becomes larger.

4.4.2.1 Parameters and behaviours of V and distributions of IBI

Contrary to the OSD model, the leaky integrate-and-fire model with a variable threshold reproduced a variety of distributions depending on the parameters. By experimenting with the parameters, we thus could reproduce the distributions of IBI of spontaneous human blinking.

When the parameters were fixed at $a = 1$, $\sigma = 0$, and $k = 0$, the mean and median values increased as c became larger within the range of 0.0–0.3 (Fig. 4.2(a)). The symmetric shape of the distribution did not change. In the leaky integrate-and-fire model, the intervals of the external input I obey a binomial distribution. Theoretically, the proposed model reproduces the normal distribution of IBI with these specific parameters because a binomial distribution with sufficient sample size approximates a normal distribution.

When the parameters were fixed at $\sigma = 0$ and $c = 0$ and then the amplitude k of the threshold functions varied in the range of 0.0–0.3, the medians of the distributions were almost constant. In this case, however, the tails of the distributions expanded and the shorter IBI showed relatively higher probability density than the longer one

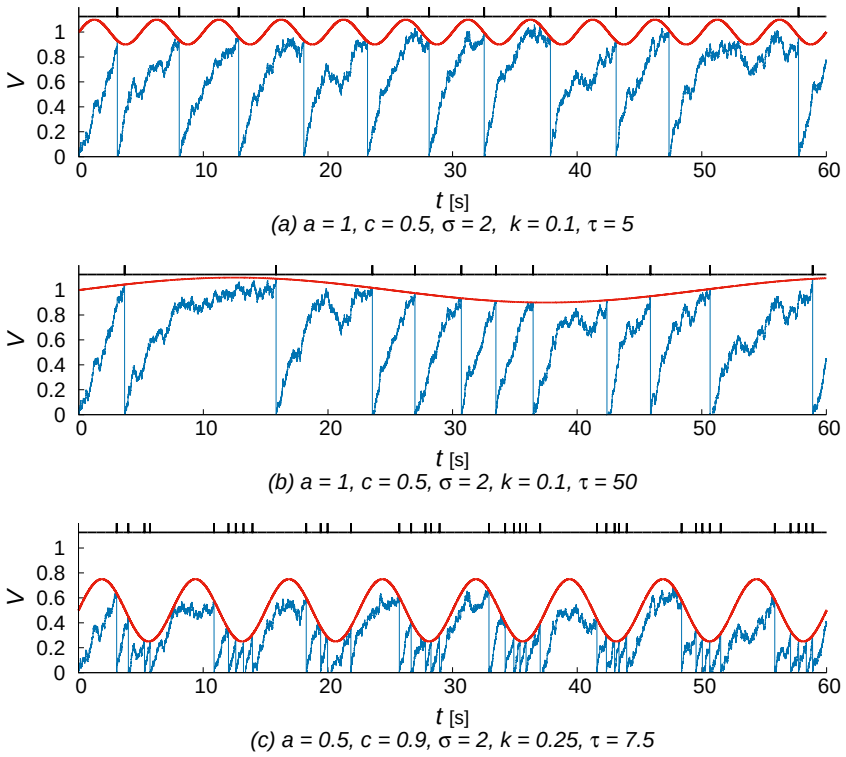

Figure 4.3: **Results by the LIF model with a variable threshold.** The V increases with integrating the binomial input I. The parameter c is the decay term and the parameter σ is the standard deviation of noise ξ. The baseline of the threshold function $a = 1$ and the threshold is time-varying with the amplitude k and the period τ. (a) The period τ is short and the prolonged IBI is observed only if the value V is not trapped by the threshold function which is convex down. (b) When the threshold function is convex up with the large period τ, the prolonged IBI is frequently observed. (c) Due to the large decay term c, the prolonged IBI is observed even when the period τ is small.

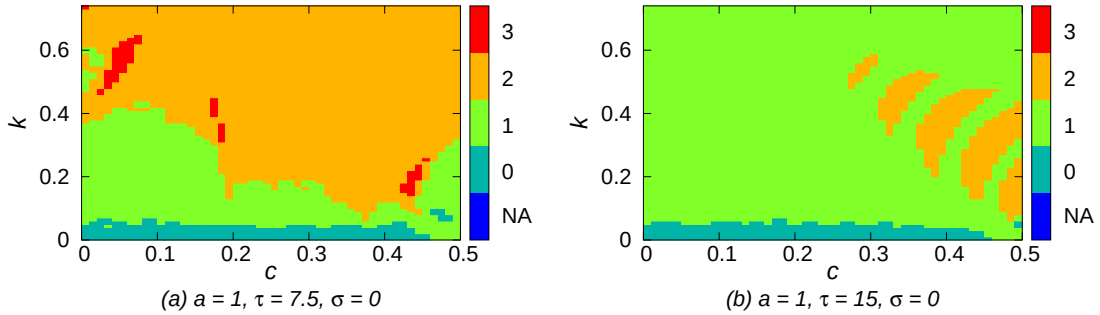

Figure 4.4: **The number of peaks of the distributions of IBI in case that c and k are changed.** The color bars show the number of peaks. (a) Trimodal distributions are observed as red clusters surrounded by the areas of bimodal distributions. (b) For the larger period τ, trimodal distributions are not observed.

(Fig. 4.2(b)).

The proposed model was capable of reproducing bimodal distributions by setting the amplitude k and the period τ of threshold functions. As shown in Fig. 4.3(a), when the threshold function $\theta(t)$ is convex downward, the value V frequently reached the threshold. In this case, the number of the peak was unity. When the threshold function $\theta(t)$ fluctuated near the baseline with a smaller amplitude and a longer period, prolonged IBIs occurred (Fig. 4.3(b)). Due to the effect of the decay term c, the value V remained just below the threshold. In this case, the number of peaks was two. Therefore, if a larger decay term was chosen, we were able to obtain both relatively longer IBIs and shorter IBIs even when the baseline was much lower (Fig. 4.3(c)).

We chose the parameters of the proposed model as shown in Table 4.2 to cover approximately widest ranges of c and k. The third column in Table 4.2 shows increments for the parameters c, k, and τ. The period $1 \leq \tau \leq 10$ s was set to correspond to the range 0.1–1.0 Hz. For the sake of simplicity, other parameters were fixed to $a = 1$ and $\sigma = 0$.

Table 4.2: Parameters used in experiments by the LIF model with a variable threshold

	range	an increment
c	[0, 1]	0.01
k	[0, 0.9]	0.01
τ	[1, 10]	0.5

In the range of these parameters, we obtained 174,629 solutions for the proposed model. The results of peak-detection showed that 4.68% (8,170/174,629) of distributions were peak-less, 37.95% (66,273/174,629) were unimodal, 41.03% (71,653/174,629) were bimodal, and 1.38% (2,411/174,629) of those were trimodal. The remaining 14.96% (26,122/174,629) of distributions were not computable due to their lower number of blinks.

The proposed model also produced trimodal distributions. Figure 4.4 demonstrates the number of peaks depending on decay term c and amplitude k when $a = 1$ and $\sigma = 0$ (these parameters are discussed in Section 4.4.2.2).

4.4.2.2 Reproduction of Ponder and Kennedy's [4] bimodal distributions of IBI

The proposed model is capable of reproducing bimodal distributions of IBIs. In this reproduction, the time bins that contain peaks were determined by the combination of baseline a and amplitude k of the threshold function $\theta(t)$. The value V is most likely to reach the threshold when the threshold function $\theta(t)$ has a minimal value at

$$\sin \frac{2\pi t}{\tau} = -1,$$

where

$$\theta(t) = a + k \sin \frac{2\pi t}{\tau} = a - k.$$

Table 4.3: Peaks and means reported in Ref. [4] and the parameter ranges to reproduce these peaks.

	Reported in Ref. [4]			Parameters of the proposed model			
Case	First peak	Second peak	Mean	$a - k$	τ	Freq.[Hz]	Median
1	0.5	3.5	2.05	$0.14 - 0.19$	$4.0 - 7.0$	$0.14 - 0.25$	$2.42 - 2.73$
2	0.5	5.0	3.31	$0.14 - 0.16$	$6.0 - 8.5$	$0.12 - 0.16$	$3.45 - 3.86$
3	0.5	5.0	3.64	$0.14 - 0.16$	$6.0 - 8.5$	$0.11 - 0.16$	$3.45 - 3.86$
4	0.5	6.5	4.12	$0.15 - 0.16$	$8.0 - 8.5$	$0.11 - 0.13$	$4.65 - 4.91$
5	1.0	5.5	3.95	$0.30 - 0.35$	$6.5 - 9.0$	$0.11 - 0.15$	$3.95 - 4.65$
6	0.5	7.0	4.45	0.15	9.0	0.11	5.03

Note. For case 6, one combination of parameters existed.

Hence, the time location of the first peaks (the peak closest to 0) is determined by the values $a - k$. If the decay term exists in the range of $0 < c < 1$, the first peak is located around 0.5 s when $a - k \simeq 0.15$. If the value V is not trapped by the threshold function, it increases with non-negative inputs. Then, the value V certainly hits the threshold function which is convex downward. Therefore, the intervals between the time location of the first peak and that of the second peak are always smaller than the period τ of the threshold function. Consequently, the time location of the second peak depends on the period τ.

Assuming that the threshold function determines time locations of peaks, we can reproduce two peaks where we intend to allocate. Table 4.3 demonstrates the time locations of peaks and the means in the bimodal distributions in the experimental study [4].

The parameters shown in Table 4.3 demonstrate the minimum value $a - k$ and the period τ that reproduce bimodal distributions. As shown in Table 4.3, $0.14 \leq a - k \leq 0.35$ and the period was $4.0 \leq \tau \leq 9.0$ s. These periods correspond to 0.11–0.25 Hz.

Furthermore, the proposed model also produces trimodal distributions if particular parameters are given. For instance, we obtain trimodal distributions when $c = 0.05$, $a = 1$, and $k = 0.6$, i.e., $a - k = 0.4$ under the condition that the period $\tau = 7.5$. The combinations of parameters that reproduce trimodal distributions were distributed as clusters (red regions in Fig. 4.4(a)). The trimodal distributions were also obtained when we expanded the ranges of parameters to $0 \leq c \leq 1$ and $0 \leq k \leq 0.9$.The trimodal distributions could exist in areas surrounded by the bimodal distributions. To reproduce the empirical bimodal distributions reported by Ponder and Kennedy [4], the parameter range of τ was estimated as 4.0–9.0. Within this range, we obtain the trimodal distributions as well.

4.5 Discussion

4.5.1 Distributions of spontaneous human blinking

Although the OSD model [41] reproduced the positively skewed, normal, and peakless distributions of spontaneous human blinking, the model did not reproduce bimodal distributions within the range of typical parameters. In contrast, the proposed model

reproduced all four distributions including the bimodal one.

Contrary to the previous experimental study [4], the positively skewed distribution was not the most common among the numerical results of the proposed model: $66,273$ cases (37.95%) followed a unimodal distributions and only $22,142$ (12.6%) cases were positively skewed. The normal distributions were also achieved by the binomial nature of inputs, albeit only in the simplest cases with noiseless inputs and thresholds with a constant value, i.e. $\sigma = 0$ and $k = 0$. In most simulations, however, $\sigma = 0$ and $k > 0$. These results suggest that a noisy system reproduces the positively skewed distributions if the threshold varies periodically. One possibility is that positively skewed distributions are common in previous studies (e.g., [50], [4]) as a consequence of the ubiquitous noise in biological systems, such as blink generators.

The bimodal distribution was also observed in the experimental study [4], albeit less commonly than the positively skewed and normal distributions. To reproduce the bimodal distributions, the differences between baseline and threshold amplitude, i.e. $a - k$, had to be set at lower values. When the value of the threshold function was convex downward (Fig. 4.3(c)), the model elicited a series of blinks within short intervals. Frequent blinking in a short period, known as "blink bursts" [41], could be explained by the short term decrease of the threshold function.

In this chapter, the proposed model also produced trimodal distributions. The combinations of the parameters that produce the trimodal distributions were not localized but distributed in small regions (Fig. 4.4). In future research, we will examine whether or not trimodal distributions of IBI can be confirmed experimentally. As one of the cases, we consider a viewing task that requires visual attentions. In such simple perceptional task, we could assume that cognitive load, i.e., I, is almost task-independent, or obey a stochastic process. The saliency and the stimulus value is well controlled and thus the visual attentions are simply regulated by the presentations of visual targets. Here, k and c could be interpreted as individual factors, sensitivity to the external stimuli and tendency to induce blink suppressions, respectively. When a participant's sensitivity is higher, this is represented as a larger value of k in the model. The parameter c is a decay term and thus if c is larger, the value V tends to fluctuate under the threshold, producing prolonged IBIs. Therefore, larger c corresponds to the tendency to induce blink suppressions.

Trimodal distributions might be observed when we change the conditional variables

that correspond to k and c in experiments with participants who show bimodal distributions. First, the targets of visual attentions are intermittently presented within 7.5 s, which corresponds to τ. Second, when a participant's sensitivity k is relatively low, e.g., $k = 0.2$, the shortest IBI would be averagely 1.6 s when there is no decay $c = 0$. Meanwhile, a participant has a moderate tendency of blink suppression, in the range of $c = 0.41 - 0.45$, trimodal distributions could be observed. For this participant, the value V fluctuates under the threshold function because decay and the input intensity are well balanced, producing prolonged IBIs. However, once the threshold is convex downward due to disappearance of targets, the value V must hit the threshold function in several hundred milliseconds, resulting a termination of the prolonged IBI. Two cases would be occurred after the reset. In one case, it takes a few seconds until the V reaches to the threshold again because the previous reset occurred approximately at the maximum value of the threshold function. In another case, short-term sequential blinking is observed if the previous reset occurred at near the minimum value of the threshold function. As the results, prolonged IBI and two types of behaviours after reset would produce the trimodal distributions of IBI.

In more complex task, k corresponds to the integration of task-dependent cognitive loads as well as individual sensitivity to the external stimuli. Thus, we need considerations on certain characteristics of the variable threshold when we argue more complex tasks by applying the proposed model.

4.5.2 The variable threshold and biological oscillations

The results of numerical simulations in this study suggest that the variable threshold plays a critical role in producing a variety of IBI distributions, especially for the bimodal distribution. Numerous experimental studies have revealed that the blink rates are regulated by internal states of the participants during performing cognitive tasks (e.g., [31], [43]). While we assumed that the variable threshold represented particular physiological fluctuations, a few plausible candidates of human internal states exist.

Researchers have reported that dopamine levels in the brain may influence IBI. For example, pathologic reduction of dopamine induces a lower frequency of blinking and fewer variations of IBI [50]. The blinking rate varies depending on the level of tonic and phasic dopamine [54]. In other words, the frequency of blinking varies in accordance with the innate baseline and transient states of the dopamine levels. As one

possibility, one could speculate that the threshold fluctuations in the proposed model correspond to phasic dopamine levels. If this hypothesis is correct, blinking frequencies increase with phasic dopamine levels, reshaping the distributions of IBI.

Rhythms of human biological systems such as brain waves [55] and attentional fluctuations [56] could also be candidates. The results of reproduction of the bimodal distributions suggested that relatively slow oscillations ($0.11-0.25$ Hz) regulate blinks. Recent neurological studies have found delta-band ($0.5-4$ Hz) blink-related oscillations (BROs) in a resting sate [57]. One study [55] reported that spontaneous blinks activate precuneus regions related to awareness and monitoring of the environment. Physiological fluctuations represented by the threshold function in the proposed model may relate to such brain waves.

4.5.3 Consistency between the model and the physiological foundations of motor control

In the proposed LIF model, V represents the changes in an internal value of a blink generator. Although the location of the blink generator circuit is controversial [50], human blinking must be involved in the general motor control circuits. There is no major contradiction if we assume that the integration of cognitive load may correspond to a direct path of excitatory motor control circuits that increase blinking frequency. On the other hand, inhibitory signals decrease blinking frequency and therefore can provide less frequent blinks, leading variations of IBI [51], [50]. The variations of the threshold would be in accordance with an indirect path of inhibitory motor control circuits. The results on IBI distributions in this paper suggest that a variable threshold can create two or three types of IBI. When we acknowledge the variable threshold in the LIF model corresponds to this inhibitory control, we can argue that human blinking rates vary in a few tens of seconds due to the effect of inhibitory signals [40]. While the LIF models are often used for a neuron, it also seems that the model would be useful to represent human blinking as the macroscopic phenomenon that involves multiple brain areas.

4.6 Conclusion

In this paper, we proposed a leaky integrate-and-fire model with a variable threshold to model human spontaneous blinking. The proposed model could reproduce the positively skewed, normal, and peak-less distributions of IBI. Moreover, the proposed model reproduced the bimodal distributions, which could not be reproduced by the OSD model at least within the typical range of parameters.

Parameters that reproduce the temporal locations of peaks in the experimental distributions reported by a classical study [4] suggest that relatively slow oscillations ($0.11 - 0.25$ Hz) govern blink elicitations. The proposed model also predicts the existence of the trimodal distributions of IBI and the distributions could be produced by the non-specific parameters. As a possible mechanism, we can assume that changes in blink rates would reflect fluctuations of threshold regulated by particular human internal states such as a brain dopamine level or rhythms of human biological system.

Trimodal distributions of IBI was numerically produced when τ is $5.0 - 7.5$ [s]. Tau was set to 5.0 [s], for instance, the variable-threshold LIF model produced trimodal distributions when the k is $0.2 - 0.4$ and decay term c is about $0.30 - 0.35$. Such combinations of parameters would be interpreted as the following conditions as physiological or psychological experiment settings. The period of threshold functions tau would correspond to a fluctuation of cognitive processing in accordance with particular external stimuli. The amplitude of the threshold function k is interpreted as the combined influence of participants' individual sensitivity to stimulus and an appeal power of stimuli. This combined influence relates to tendency to occur short-term sequential blinking because $a - k$ is the minimum value of threshold function that determines the shortest intervals of blinking. The decay term c is interpreted as an individual factor that regulates internal state value in the balance of an external input, eliciting a blink suppression.

As one of the cases but not limited, if we consider a viewing task that requires visual attentions, the conditions of parameters could be interpreted in the experimental settings as follows. In this setting, it could be assumed that an appeal power of the stimuli is approximately constant because the saliency or the stimulus value are well controlled. Hence, the k simply corresponds to individual sensitivity to stimulus in this context. Regarding the case that an appeal power is dominant, see Chapter 2.

First, the target of the visual attention appears intermittently between $5.0 - 7.5$ [s] corresponding to τ. Second, the participant's sensitivity k is $0.2 - 0.4$. This means that the shortest IBI would be averagely $1.2 - 1.6$ [s] when there is no blink suppression, i.e., $c = 0$. Meanwhile, a participant has the tendency of relatively weak blink suppression, i.e., c is $0.30 - 0.35$, the internal state value fluctuates under the threshold function because decay and the input intensity are well balanced, resulting in prolonged intervals of blinking. However, once the threshold is convex downward, e.g., due to disappearance of target stimuli, the internal state value must reach to the threshold function in several hundred milliseconds, resulting a termination of the prolonged IBI. Two cases would be considered after the reset. In one case, it takes few seconds until the internal state value reaches to the threshold again because the previous reset occurred approximately at the maximum value of the threshold function. In another case, short-term sequential blinking is observed if the previous reset occurred at near the minimum value of the threshold function. As the results, prolonged IBI and two type of behaviours after reset would produce the trimodal distributions IBI. The adequacy of the variable-threshold LIF model of human blinking is tested by examining whether or not the trimodal distributions are observed in the future experiments.

Chapter 5

Reconstruction of common input with using superposed recurrence plots

5.1 Introduction

Biological systems receive inputs from external environment. In microscopic level, for instance, neurons throughout our body receive intermittent inputs. Common inputs transmit information by changing the behavior of the forced biological systems, and thus play certain roles in communications among biological systems. However, the amplitude of common inputs in each time are usually not known for an observer. Direct observations of the common inputs are frequently not easy for researchers because the measurement of signals per se often influences on the behaviors of biological systems. Thus, reconstructing a common input by using the observed behaviors is one of the important issues of time series analysis on various biological systems. In this chapter, I propose a reconstructing method common inputs for point processes.

As shown in Chapter 4, the proposed model is assumed as leaky integrate-and-fire model with a variable-threshold for spontaneous blinking. Because the fluctuations of threshold can be mathematically transformed to a modulation of the input, the model also indicates that fluctuations of common input would change blink rates of each audience member. Thus, a variety of distributions shown in Chapter 4 can be by driven the common input. To reveal such external inputs, reconstruction of time series

using recurrence plots [2] is one of the strong non-linear methods.

The purpose of this chapter is to propose a method to reconstruct time series of common input using point process data and the examine the precision of the reconstructed time series. For this aim, I use the number of firings per unit time, i.e., firing rates, of Izhikevich neuron model as a good example to produce occurrence numbers time series within each time window. By changing parameters, Izhikevich neuron model can exhibit a variety of firing patterns such as Regular Spiking (RS), Chattering Spiking (CH), Fast Spiking (FS), and others. If the method can be used for a firing rates time series, then I apply this method to the number of blinks per unit time, i.e., blinking rates, as well.

5.2 Reconstruction of common input

5.2.1 Recurrence plots and forced dynamical system

Dynamical systems often show recurrences. In other words, a state of some dynamical system returns to the former state along with the similar trajectory in phase space. Recurrence plots are two-dimensional visualizations of this nature. Based on Takens's embedding theorem [58], embedding of time series to a time delay coordinates system was established as the basic method to construct multidimensional dynamics in phase space from an observed variable.

In 1987, using this embedding method, Eckmann [59] proposed a recurrence plot as a method to visualize a nonlinearity and nonstationarity of an observed time series. Subsequently, recurrence plots were used to reveal the characteristics of time series obtained from dynamical system. Ten years later, however, Casdagli [60] demonstrated that a recurrence plot of which embedding dimension is sufficiently large shows similar patterns with the recurrence plot of a common input as long as the common input change slowly and smoothly.

After this revisit, recurrence plots became to be recognized as the method to describe the dynamics of inputs. Thus, the recurrence plots have been used for estimating of underlying dynamical system. Using visual features of recurrence plots, several quantification indices for time series analyses have been developed [61]. For example, *DET* is used for detecting determinism because the diagonal components are observed in

recurrence plots when the driving system have determinism. In recent years, quantification methods based on recurrence plots are also applied to detect the relationships between biological signals in physiological data [62] and semantic networks in human group dynamics [63].

Another application of recurrence plots is to estimate the common input time series. Although recurrence plot is a two-dimensional visualization, the distances between one state and another state possess the underlying dynamics of a high dimensional phase space. Thus, it contains whole information to reconstruct the input. As shown by Casdagli [60], the recurrence plots of forced system are similar with that of the common inputs when we embed a forced system to time delay coordinates in sufficiently high dimensions. This is because that both states of forcing system and the forced system are simultaneously neighboring each other when the neighboring points exist in the time delay coordinates. Thus, we can obtain a time series of the common input by transforming the union of recurrence plots calculated using observed forced systems because the recurrence plots are a subset of the recurrence plots of the inputs [2].

Although Casdagli [60] pointed out that an input can be reconstruct as long as it changes slowly and smoothly, Hirata et al. [2] demonstrated that the input can be reconstructed when we can observe multiple forced systems based on Stark's embedding theorem which consider real situations in experiments and natural settings. Stark's embedding theorem [64] assume that system is driven by the other system while Takens's embedding theorem assume that underlying system is autonomous. Because respective recurrence plots of forced systems are subsets of the recurrence plots of the common input, the unique parts of each recurrence plot are removed and thus the union corresponds to the inputs when we take a union of the recurrence plots of forced systems. Thus, we can reconstruct time series of the input when we have no prior knowledge if we can observe multiple systems [2], with using the network-based method that proposed by Sauer [65].

However, physiological experiments often provide point process data, such as the firing intervals of a single neuron. Time series analyses using recurrence plots were also applied to the point process data [66]. This study also reported that recurrence plots of firing rates can reconstruct the original recurrence plot of the input signal, even when neurons show chaotic firing characteristics as well as they show a periodical firing pattern. Based on these results, it is suggested that the time series of the common

input would be reconstructed by using firing rates of the neurons that receive the forcing common input [2]. However, it remains unknown how much we can reconstruct the common input by using firing rates time series of neuron model and whether we can apply the method to the data of human blinking.

In this chapter, I aim to examine efficacy of the reconstructing method for point processes. First, I introduce the reconstructing method and propose a method using superposed recurrence plots to reconstruct time series of a common input. Then, I examine the precision of the reconstructed time series. Finally, to reconstruct the time series of common input that corresponds expressive performance, I apply the method to the blinking rates, i.e., the number of blinks per unit time.

5.2.2 Superposed recurrence plot with using multiple firing rates

Suppose y_t be states at time t sampled within each time interval of τ and one-dimensional observation function φ: $A \to \mathbb{R}$. Based on Takens Theorem [58], if we take a observable $\varphi(y_t)$, which is mapped on the d-dimensional coordinates, we can obtain a reconstructed copy of the original system as

$$(\varphi(y_t),\ \varphi(y_{t+\tau}),\ \varphi(y_{t+2\tau}), \ldots, \varphi(y_{t+(d-1)\tau})). \tag{5.1}$$

Stark [64] expanded this Takens Theorem. Stark's version of embedding theorem [64] assume that a system is driven by another system. Suppose $f\colon A \to A$ be a dynamical map on a m-dimensional manifold and $g\colon Q \to Q$ be a dynamical map on a n-dimensional manifold. A dynamical system on $A \times Q$ is described as

$$x(t+1) = f(x(t), y(t)), \tag{5.2}$$

and

$$y(t+1) = g(y(t)), \tag{5.3}$$

where $x(t)$ represents the state of the forced system and the map g represents a forcing system. Thus, using the current state $(x(t),\ y(t))$, the next state is defined as $(\ x(t+1),\ y(t+1)\ ) = (\ f(x(t),\ y(t)),\ g(y(t))\ )$. Furthermore, we can define the map $\Phi_{f,g,\varphi}$

applying φ:

$$\Phi_{f,g,\varphi}(x,y) = (\ \varphi(f^{(0)}(x,y)),\ \ \varphi(f^{(1)}(x,y)),\ldots,\varphi(f^{(d-1)}(x,y))\ ), \tag{5.4}$$

where the maps are given by $g^{(0)}(y) = y$, $g^{(i+1)}(y) = g(g^{(i)}(y))$, $f^{(0)}(x,y) = x$, and $f^{(i+1)}(x,y) = f(f^{(i)}(x,y), g^{(i)}(y))$. Stark's version of Takens Theorem says that $\Phi_{f,g,\varphi}$ embeds (A,Q) into $\mathbb{R}^d$ under the condition of $d \geq 2(m+n)+1$.

In the reconstructing method [2], Hirata prepared multiple forced systems to take the union of recurrence plots. In this set up, suppose $f\colon A_\kappa \to A_\kappa$ be dynamical maps on a m_κ-dimensional manifold for κth system ($\kappa = 1, 2, \cdots, K$). As the extension of above theoretical considerations, the states of system x_κ and y are modeled by the following equations:

$$x_\kappa(t+1) = f_\kappa(x_\kappa(t), y(t)), \tag{5.5}$$

and

$$y(t+1) = g(y(t)). \tag{5.6}$$

For these equations, using the current state $(x_\kappa(t), y(t))$, the next state is defined as $(\ x_\kappa(t+1),\ \ y(t+1)\ ) = (\ f_\kappa(x_\kappa(t), y(t)),\ g(y(t))\ )$. Thus, we can define the maps $\Phi_{f_\kappa,g,\varphi}$ applying φ for each κ:

$$\Phi_{f_\kappa,g,\varphi}(x_\kappa,y) = (\ \varphi(f_\kappa^{(0)}(x_\kappa,y)),\ \ \varphi(f_\kappa^{(1)}(x_\kappa,y)),\ldots,\varphi(f_\kappa^{(d-1)}(x_\kappa,y))\ ). \tag{5.7}$$

Subsequently, Hirata's extension of Takens Theorem says that $\Phi_{f_\kappa,g,\varphi}$ embeds (A_κ, Q) into $\mathbb{R}^d$ under the condition of $d \geq 2(m_\kappa + n) + 1$. Henceforth, we describe $\Phi_{t,\kappa}$ the value of $\Phi_{f_\kappa,g,\varphi}(x, y_\kappa)$ at time t for notational convenience.

Let $\boldsymbol{R}_{ij,\kappa}(\epsilon_\kappa)$ be an $T \times T$ recurrence matrix defined as

$$\boldsymbol{R}_{ij,\kappa}(\epsilon_\kappa) = \Theta(\epsilon - \|\Phi_{i,\kappa} - \Phi_{j,\kappa}\|), \quad i = 1,2,\ldots,T, \quad j = 1,2,\ldots,T, \tag{5.8}$$

where ϵ_κ is a threshold distance, and $\Theta(\cdot)$ is the Heaviside step function. While Heaviside function returns one if $\|\Phi_{i,\kappa} - \Phi_{j,\kappa}\| < \epsilon$, it returns zero otherwise. Recurrence plot is a visualization of this matrix in which the ones are plotted as black and zeros are plotted as white.

To interpolate the information of common input, we overlapped these multiple

recurrence plots $\boldsymbol{R}_{ij,\kappa}(\epsilon_\kappa)$. To calculate this recurrence plots, we suppose a $T \times T$ recurrence matrix which is defined using the mathematical expression:

$$\boldsymbol{SR}_{ij}(\epsilon_1, \ldots, \epsilon_K) = \sum_{\kappa=1}^{K} \boldsymbol{R}_{ij,\kappa}(\epsilon_\kappa), \quad i = 1, 2, \ldots, T, \quad j = 1, 2, \ldots, T, \tag{5.9}$$

where ϵ_κ is the threshold for κ system $x_1,\ x_2,\ \ldots,\ x_K$. In this study, the ϵ_κ for each system were determined as the number that corresponds to the lower 10 % of the total number of combinations between i and j. We refer $\boldsymbol{SR}_{ij}(\epsilon_1, \ldots, \epsilon_K)$ as superposed recurrence plot in this thesis.

5.2.3 Reconstruction procedures using recurrence plots

In Ref. [2], Hirata et al. proposed a method to reconstruct a common input using recurrence plots. A recurrence plot is visual representation using two-dimensional matrix in which the ones dot as black and zeros dot as white.

With using the threshold ϵ^κ, we put a dot on $\boldsymbol{R}_{ij,\kappa}$ for each κ. Then, the $\boldsymbol{SR}_{ij}(\epsilon_1, \ldots, \epsilon_K)$ is transformed to a binarized superposed recurrence plot by using the threshold q of binarization. If we set $q = 1$, the dots were put when the value of $\boldsymbol{SR}_{ij}(\epsilon_1, \ldots, \epsilon_K)$ was more than one. This means that dots (i, j) in the binarized recurrence plot were plotted when at least one point exists on (i, j) in $\boldsymbol{R}_{ij,\kappa}$.

Next, we calculate a weight for each link using the G_i as the set of time indices to which i is close. Regarding each existing edge between i and j, the weight W was defined as

$$W(i, j) = 1 - \frac{|G_i \cap G_j|}{|G_i \cup G_j|}, \tag{5.10}$$

where $|X|$ means the number of elements in set X, the signs $\cap$ and $\cup$ show the intersection of two sets and the union of two sets, respectively. The weight of the link corresponds the distance between states x_i and x_j. Thus, the minimum of Eq. 5.2.3 is zero when $G_i = G_j$. We define a set of link weights corresponding the pair of i and j as the distance matrix D_{ij}.

In Ref. [2], Hirata et al. detected the structure of the network by finding shortest paths among all pairs of i and j. Finally, the original time series is reconstructed by applying a method of multidimensional scale to the shortest path matrix d. However,

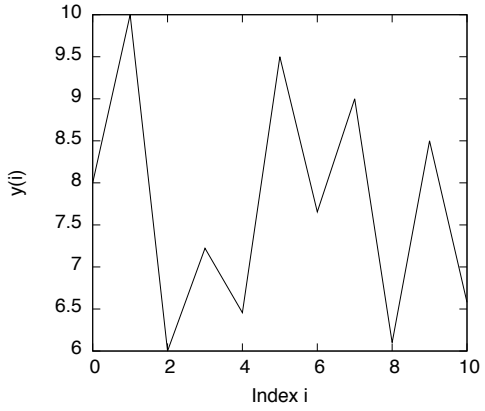

(a) Original time series

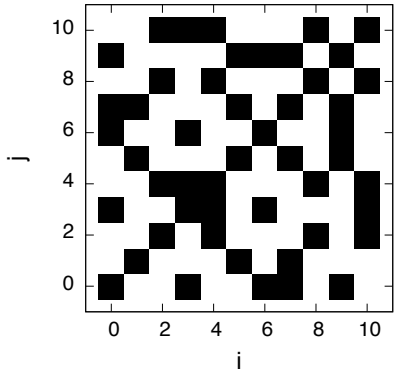

(b) A recurrence plot of the time series

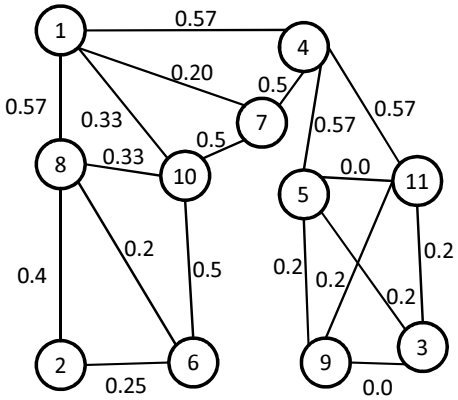

(c) A network created using the recurrence matrix(b)

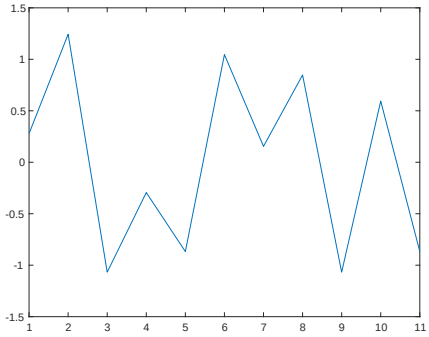

(d) Reconstructed time series

Figure 5.1: **Reconstruction of a time series [2]** (a) An example of original time series. (b) Recurrence plot of the data of (a) using $\theta = 0.3$. (c) a network presentation of a weight matrix D_{ij}. The weight 0.0 means that the two time indcies are identical and thus they are indistinguishable twins [2]. (d) Reconstructed time series obtained as the results of the multidimensional scaling method.

I utilized only the distance matrix D_{ij} as the structure of time series in the following estimations of embedding parameters.

As an example of this method, I show the reconstruction of a toy time series like X of Duffing equation. Based on the recurrence plot in Fig. 5.1, I calculated D_{ij}. In this matrix D_{ij}, the sign "–" shows that there is no direct path.

$$D_{ij} = \begin{pmatrix}
0.00 & – & – & 0.57 & – & – & 0.2 & 0.57 & – & 0.33 & – \\
– & 0.00 & – & – & – & 0.25 & – & 0.4 & – & – & – \\
– & – & 0.00 & – & 0.20 & – & – & – & 0.00 & – & 0.20 \\
0.57 & – & – & 0.00 & 0.57 & – & 0.50 & – & – & – & 0.57 \\
– & – & 0.2 & 0.57 & 0.00 & – & – & – & 0.20 & – & 0.00 \\
– & 0.25 & – & – & – & 0.00 & – & 0.20 & – & 0.50 & – \\
0.20 & – & – & 0.50 & – & – & 0.00 & – & – & 0.50 & – \\
0.57 & 0.40 & – & – & – & 0.20 & – & 0.00 & – & 0.33 & – \\
– & – & 0.00 & – & 0.20 & – & – & – & 0.00 & – & 0.20 \\
0.33 & – & – & – & – & 0.50 & 0.50 & 0.33 & – & 0.00 & – \\
– & – & 0.20 & 0.57 & 0.00 & – & – & – & 0.20 & – & 0.00
\end{pmatrix}$$

Then, we can obtain an $i \times i$ shortest path matrix d. The matrix of the shortest paths d was as follows:

$$d = \begin{pmatrix}
0.00 & 0.97 & 1.34 & 0.57 & 1.14 & 0.77 & 0.20 & 0.57 & 1.34 & 0.33 & 1.14 \\
0.97 & 0.00 & 2.31 & 1.54 & 2.11 & 0.25 & 1.17 & 0.40 & 2.31 & 0.73 & 2.11 \\
1.34 & 2.31 & 0.00 & 0.77 & 0.20 & 2.11 & 1.27 & 1.91 & 0.00 & 1.68 & 0.20 \\
0.57 & 1.54 & 0.77 & 0.00 & 0.57 & 1.34 & 0.50 & 1.14 & 0.77 & 0.90 & 0.57 \\
1.14 & 2.11 & 0.20 & 0.57 & 0.00 & 1.91 & 1.07 & 1.71 & 0.20 & 1.48 & 0.00 \\
0.77 & 0.25 & 2.11 & 1.34 & 1.91 & 0.00 & 0.97 & 0.20 & 2.11 & 0.50 & 1.91 \\
0.20 & 1.17 & 1.27 & 0.50 & 1.07 & 0.97 & 0.00 & 0.77 & 1.27 & 0.50 & 1.07 \\
0.57 & 0.40 & 1.91 & 1.14 & 1.71 & 0.20 & 0.77 & 0.00 & 1.91 & 0.33 & 1.71 \\
1.34 & 2.31 & 0.00 & 0.77 & 0.20 & 2.11 & 1.27 & 1.91 & 0.00 & 1.68 & 0.20 \\
0.33 & 0.73 & 1.68 & 0.90 & 1.48 & 0.50 & 0.50 & 0.33 & 1.68 & 0.00 & 1.48 \\
1.14 & 2.11 & 0.20 & 0.57 & 0.00 & 1.91 & 1.07 & 1.71 & 0.20 & 1.48 & 0.00
\end{pmatrix}$$

The original time series (Fig. 5.1(a)) was reconstructed using a recurrence plot Fig. 5.1(d)). Because a recurrence plot is symmetry with respect to the main diagonal, only an upper or a lower triangular matrix is used for calculations of weight. As shown in Fig. 5.1(a) and (d), the reconstructed time series maintained almost all information, except for scale factor of a time series.

5.3 Common input to Izhikevich neuron model with slightly different parameters

5.3.1 Recurrence plot using firing rates of a single neuron

To test the reconstructing method by using superposed recurrence plots relatively slow and smooth common input was suitable. Figure 5.2(a)-(b) show a time series of a common input which was generated by Duffing equation and its recurrence plot. In this recurrence plot, the plotted lines and blocks shows smooth because the time series vary in a relatively slow way. As a common input, we used the values of a variable X of Duffing equation. Duffing equation is defined as

$$\begin{cases} \dot{x} &= y \\ \dot{y} &= -0.05y - x^3 + 7.5\cos t. \end{cases} \tag{5.11}$$

Figure 5.2(a) shows an original time series of a common input which was generated from Duffing equation. For recurrence plot, 6,000 points were sub-sampled in each 10 point from this time series. Figure 5.2(b) demonstrates a recurrence plot of the common input.

We selected Izhikevich neuron model because it can reproduce various firing patterns with substantially different baselines of firing rates just by changing the parameters. Izhikevich neuron model of a neuron is described as follows:

$$\begin{cases} \dot{v} &= 0.04v^2 + 5v + 140 - u + I_v(t) \\ \dot{u} &= a(bv - u) \end{cases} \tag{5.12}$$

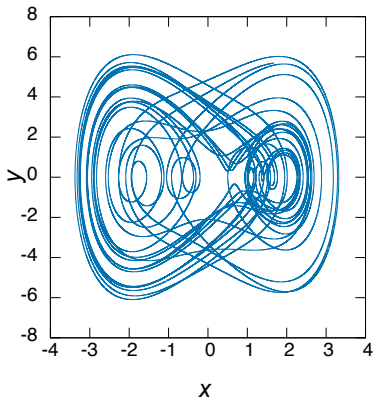

(a) A solution of Duffing equation solved by Runge-Kutta method

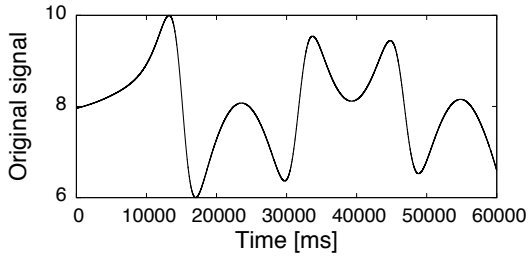

(b) Time series of common input (re-scaled)

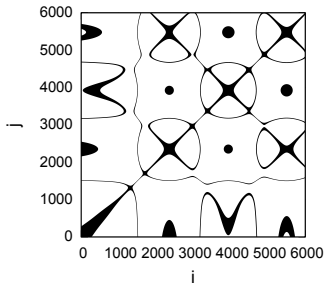

(c) Recurrence plot of common input

Figure 5.2: **Original time series of common input and its recurrence plot.** (a) Duffing equation. (b) The first 60,000 points of variable x of Duffing equation were plotted. (c) A recurrence plot of 6,000 points sampled in each 10 point from the time series (b). The parameters embedding dimension $m = 5$ and the delay time $\tau = 1$ were used.

$$\text{if} \quad v \geq 30, \quad \text{then} \begin{cases} v \leftarrow c \\ u \leftarrow u + d, \end{cases}$$

where v is the membrane potential, u is the recovery variable, and $I_v(t)$ is the forcing input. Other parameters a, b, c, and d determine the firing pattern of the neuron.

To test whether or not a recurrence plot can reconstruct the time series of the common input, we apply the method to a firing rates time series calculated by single Izhikevich neuron model. First we generated three Regular Spiking models with the parameters $0.018 \leq a \leq 0.022$ and $0.198 \leq b \leq 0.202$. Figures 5.3(a)–(c) demonstrated that the recurrence plots by using firing rates of Regular Spiking models which are driven by the common input (Fig. 5.2(a)). As shown in Figure 5.3(a)–(c), the rough patterns of the recurrence plots were similar with each other. These recurrence plots also shared similar features with the recurrence plot of the common input.

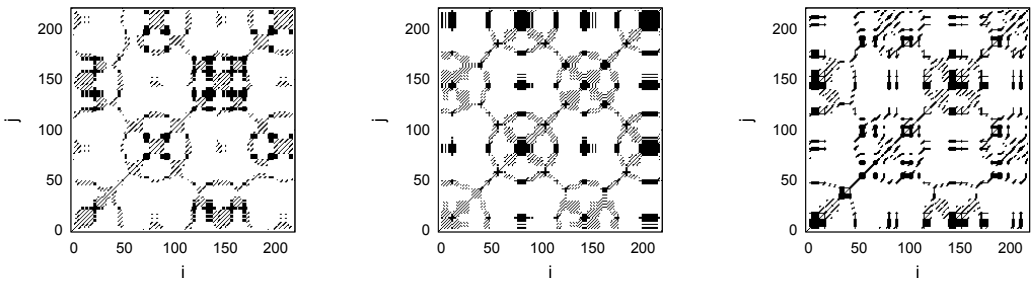

(a) $a = 0.020$, $b = 0.200$, $c = 65$ $d = 8$. (Parameters of Regular Spiking in Ref. [67])

(b) $a = 0.018$, $b = 0.198$, $c = 65$ $d = 8$.

(c) $a = 0.022$, $b = 0.202$, $c = 65$ $d = 8$.

Figure 5.3: **Recurrence plots using firing rates of Izhikevich models with slightly different parameters that exhibit Regular Spiking.** Width of time windows $w = 1000$.

However, these recurrence plots calculated using the firing rates of single neurons could not reconstruct the time series of common inputs. This due to the fact that a recurrence plot using the firing numbers of the single neurons contains both dynamics of common input and the neuron model. We cannot separate these information, and thus we would lose information of common input as long as using the responses of single neuron.

Hence, we propose a method to interpolate information by taking a union of multiple

recurrence plots to obtain the shared recurrences. Firing rates of a neuron approximately corresponds to the amplitude of the common input. Thus, in the case that we impose a common input to the neurons with individual differences, the number of firings increases at the approximately same timing while the precise values of firing rates differ with each other. From these variations firing rates, we can obtain different though partially overlapping patterns of recurrence plots. By taking the union of recurrence plots, the unique dynamics of each neuron would be canceled with each other, and thus we would be able to obtain the component of the common input.

5.3.2 Reconstruction of common input with using superposed recurrence plots

5.3.2.1 Superposed recurrence plots of firing rates obtained from neurons that exhibit particular firing patters

We generated 80 models that exhibit Regular Spiking with the parameters $0.018 \leq a \leq 0.022$ and $0.198 \leq b \leq 0.202$. Figures 5.4(a)-(c) demonstrated that superposed recurrence plots by using firing rates of these models which are driven by the common input. When $w = 500$ and $w = 1000$, the rough patterns of the recurrence plots were similar with each other. These recurrence plots also shared similar features with the recurrence plot of the common input.

To test the results of Chattering and Fast Spiking models are consistent with that of Regular Spiking models, we generated 80 models by changing parameters a and b. Then, we added the common input (Fig. 5.2(a)) to these models. Figure 5.4 shows the superposed recurrence plots calculated by using firing rates of Chattering and Fast Spiking models. Regarding Chattering Spiking models, the patterns of recurrence plots were similar with that of Regular Spiking as well as the common input when the width of time window $w = 500$ and $w = 1000$. Unlike the results of Regular Spiking and Chattering Spiking, the line widths in recurrence plots were narrow.

For Regular Spiking and Chattering Spiking, when I used 100 [ms] time window for calculating the firing rates, I cannot reconstruct the time series of the common input because the almost all superposed recurrence plots were filled with black points. By contrast, for Fast Spiking, I can reconstruct a time series, whilst the shapes are different from the original common input if the embedding dimension $m = 1$ or $m = 3$

when I used the 100 [ms] time window.

For Regular Spiking and Chattering Spiking, when I used 500 [ms] time window for calculating the firing rates, I can obtain the time series from the superposed recurrence plots, and the shape became smoother when the embedding dimension became larger. When I use 500 [ms] time window for firing rate from Fast Spiking, we can reconstruct smooth and almost exact time series of the common input even when $m = 1$ or $m = 3$, yielding a fewer root mean square errors.

When I used 1000 [ms] time window for calculating the firing rates obtained from Regular Spiking and Chattering Spiking, while I can obtain the time series, the time series had small fluctuations than that obtained when I used 500 [ms] time window. By contrast, firing rate obtained from Fast Spiking can reconstruct the time series of the common input and the root mean square errors were small, approximately 0.1. The absolute values of maximal values and minimal values is smaller than that obtained when I used 500 [ms] time window, resulting larger errors.

Then, we examined the relations between embedding dimension and ability of reconstruction. Figure 5.5 shows the differences between the original time series of the common input and the reconstructed time series when we used Regular Spiking and Fast Spiking. As shown in Fig. 5.5, in the case of embedding dimension $m = 1$ indicating that no embedding was done, the time series of the common input were not reconstructed when we used Regular Spiking neurons.

Finally, to evaluate precision of reconstruction, we calculated the root mean square errors (RMSE) of each width of time window and embedding dimensions.

In sum, when I used firing rates obtained from Fast Spiking, compared to that from Regular and Chattering Spiking, the precisions of the reconstructed time series were higher.

The baseline firing rates were 15, 60, and 80[spikes/sec] for Regular, Chattering, and Fast Spiking, respectively. When the firing rates baseline is higher, the forced Izhikevich neurons can reflect the variations the common input. Thus, these results would due to the higher firing rates baseline of Fast Spiking which possess higher temporal resolution to the forcing input.

Then, I examined the binarizing-threshold q dependency of the reconstructing method using superposed recurrence plots. Left panels of Fig. 5.7 show the binarized superposed recurrence plots with the threshold (a) $q = 1$, (c) $q = 8$, (e) $q = 32$, and (e)

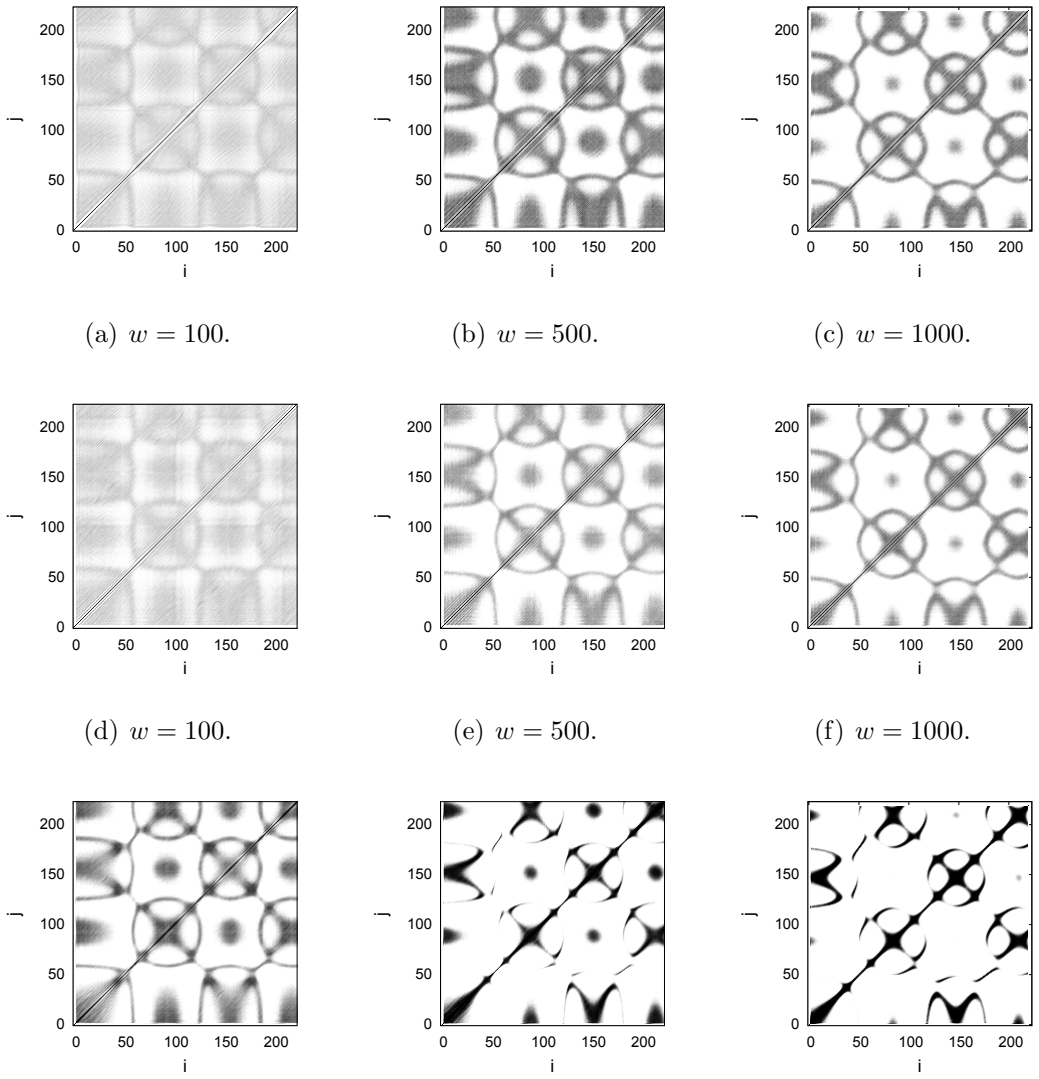

(a) $w = 100$. (b) $w = 500$. (c) $w = 1000$.

(d) $w = 100$. (e) $w = 500$. (f) $w = 1000$.

(g) $w = 100$. (h) $w = 500$. (i) $w = 1000$.

Figure 5.4: **Superposed recurrence plots using the firing rates of (a)–(c) Regular Spiking, (d)–(f) Chattering Spiking, and (g)–(i) Fast Spiking models.** The embedding dimension $m = 5$ and time delay $\tau = 1$. The ws are the width of time window for calculations of firing rates.

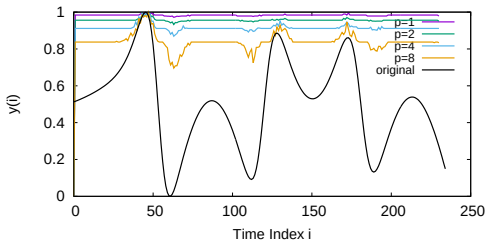

(a) RS, $m = 1$.

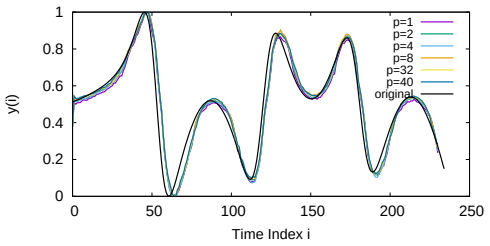

(b) FS, $m = 1$.

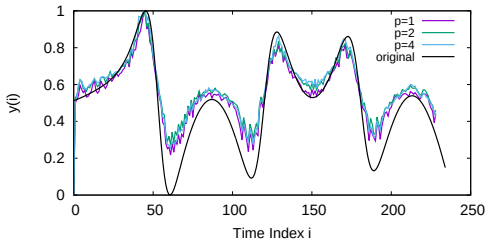

(c) RS, $m = 3$.

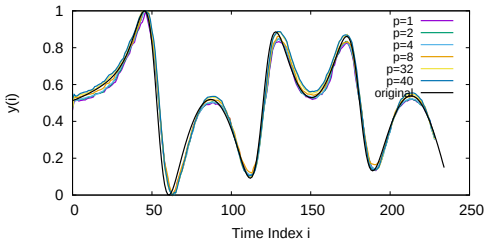

(d) FS, $m = 3$.

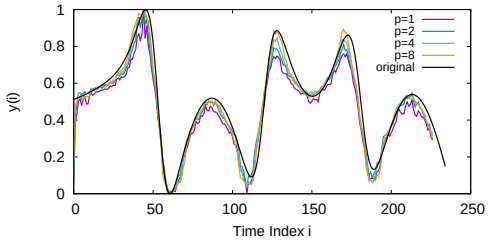

(e) RS, $m = 5$.

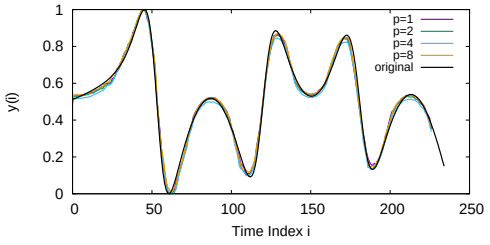

(f) FS, $m = 5$.

Figure 5.5: **Root mean square error depending on embedding dimension m and threshold of superposed recurrence plots p.** Width of time window $w = 500$.

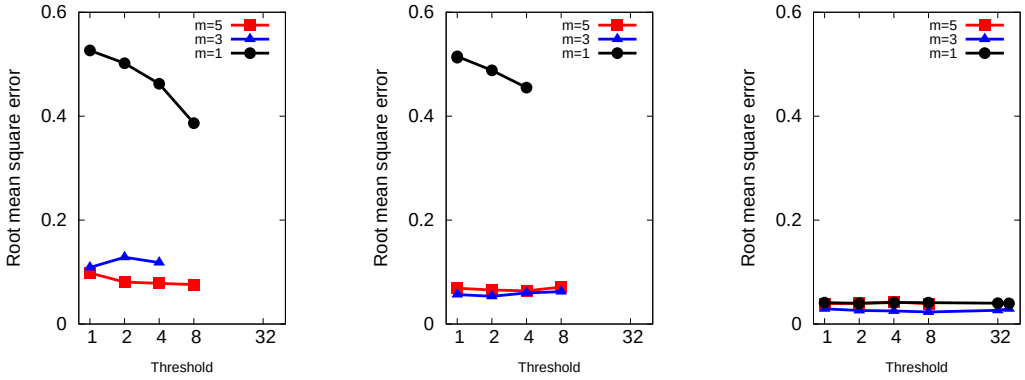

(a) Regular Spiking. $w = 500$.

(b) Chattering Spiking. $w = 500$.

(c) Fast Spiking. $w = 500$.

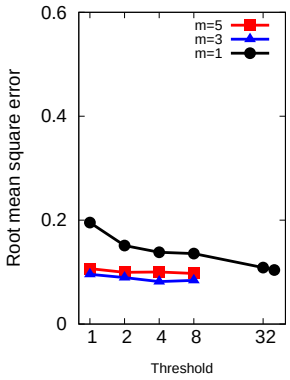

(d) Regular Spiking. $w = 1000$.

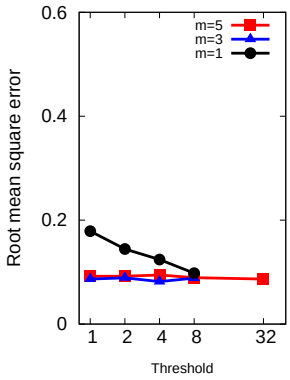

(e) Chattering Spiking. $w = 1000$.

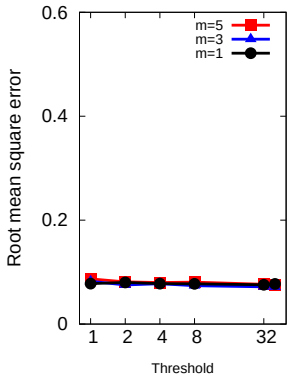

(f) Fast Spiking. $w = 1000$.

Figure 5.6: **Root mean square errors for embedding dimension m and threshold of superposed recurrence plots for Regular, Chattering, and Fast Spiking.** When $m = 1$, original firing rates time series were used, i.e., embedding was not applied.

$q = 40$. Right panels of Fig. 5.7 show the reconstructed time series by using binarized superposed recurrence plots with the threshold (b) $q = 1$, (d) $q = 8$, and (f) $q = 32$. When we used the threshold $q = 40$, the half number of cumulations, the method could not be applied because the distances between each point were incomputable.

5.3.2.2 Superposed recurrence plots of firing rates obtained from different models

The models shown in Section 5.2.2 have different baselines of firing rates: The baseline firing rates were 15[spikes/sec] for Regular Spiking, 60[spikes/sec] for Chattering Spiking, and 80[spikes/sec] for Fast Spiking. Nonetheless, we can reconstruct the time series of the common input using firing rates time series obtained from each firing patterns as long as the embedding dimensions were sufficiently high and the widths of time window is appropriate. Because the rough shapes of recurrence plots generated by using these firing rates were similar with each other, I conclude that the differences of mean firing rates have little influence on rough shapes of recurrence plots when we use the distance in embedded spaces.

Therefore, there exits a possibility that the recurrence plots have partial information of the recurrence plot of the common input, regardless of the baseline firing rates of forced neuron models. If this is plausible, information of the common input would be captured even when the reconstructing method is applied to the combinations of multiple firing patterns of Regular, Chattering, and Fast Spiking. To test this hypothesis, I generated 80 models by changing parameters a and b of Izhikevich models that exhibit Regular Spiking, Chattering Spiking, and Fast Spiking. Then, in ascending order of parameters, we chose first 27 models, middle 27 models, and last 26 models out of 80 models of respective firing patterns. Then, we added the common input (Fig. 5.2(a)) to these models. Figures 5.8(a)–(c) show the resulting recurrence plots of (a) Regular, Chattering, and Fast Spiking, (b) Chattering, Fast, and Regular Spiking, and (c) Fast, Regular, and Chattering Spiking.

As shown in Fig. 5.8(a)–(c), the superposed recurrence plots calculated by using firing rates of Regular, Chattering, and Fast Spiking were similar with each other. The shared rough shapes were similar to that of the common input as well.

I also applied the method to the recurrence plot calculated by using firing rates of first 27 Regular Spiking, middle 27 Chattering Spiking, and last 26 Fast Spiking

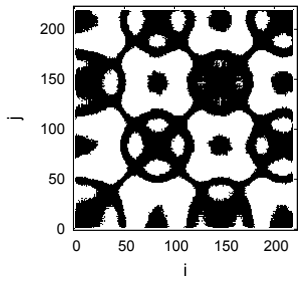

(a) $q = 1$.

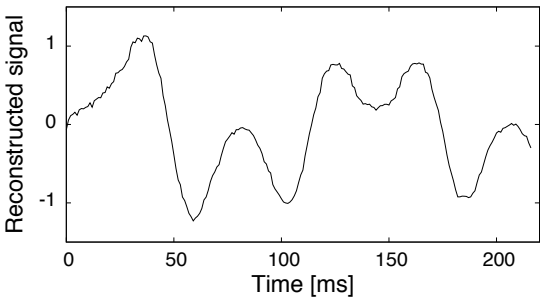

(b) Reconstructed time series when $q = 1$.

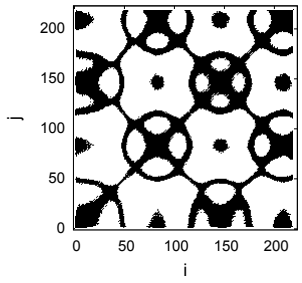

(c) $q = 8$.

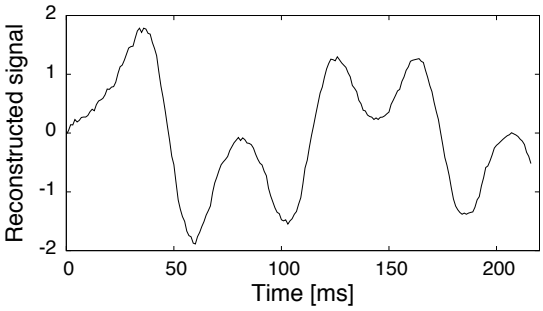

(d) Reconstructed time series when $q = 8$.

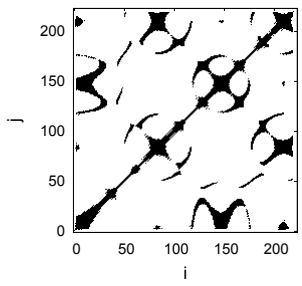

(e) $q = 32$.

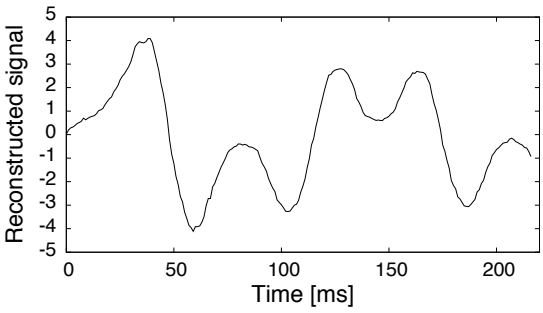

(f) Reconstructed time series when $q = 32$.

Figure 5.7: **Binarized superposed recurrence plots and reconstructed time series.**

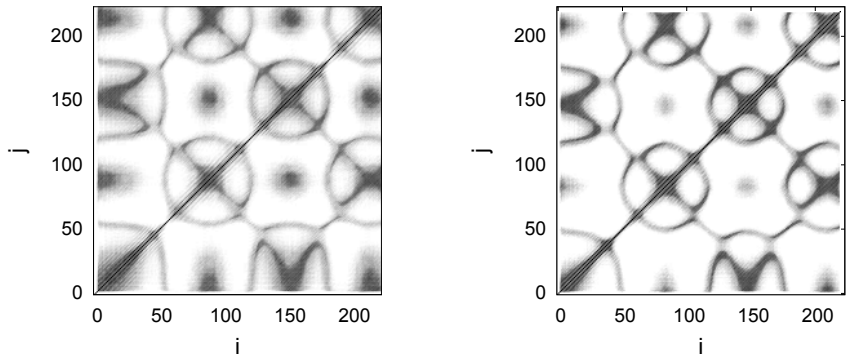

(a) RS, CH, and FS.$ws = 500$. (b) RS, CH, and FS.$ws = 1000$.

Figure 5.8: **Superposed recurrence plots by using mixture of firing rates time series of each firing pattern.** RS: Regular Spiking, CH: Chattering Spiking, and FS: Fast Spiking. Width of time window $w = 500$ and $w = 1000$.

models chosen from 80 models with slightly different parameters. This combination corresponds to Fig. 5.8(b). As shown in Fig. 5.7, the common input was able to be reconstructed using the superposed recurrence plots. When the threshold q became larger, the common inputs were reconstructed as a smoother line while the precisions were nearly independent of the threshold. When the threshold $q = 40$, however, we could not obtain a reconstructed time series. This would be due to the fact that the dominant lines on the superposed recurrence plots disappeared.

By using the proposed superposed recurrence plots, I can reconstruct the time series of the common input while the forced system outputs are point process data. Totally, the precisions became better when the embedding dimensions were higher.

According to Casdagli [60], recurrence plots can detect the common input as long as it is smooth and slow. Thus, time scale would influence on these results. The time series of the common input was more precisely reconstructed in case the firing rates are high enough compared to the variations of the common input. Therefore, I can point out that the possibility that firing rates time series obtained from Regular Spiking or Chattering Spiking neurons can reconstruct the common input in lower embedding dimensions when the time scale of Duffing equation is changed to be more slowly.

However, from the theoretical view, the information of each firing rates time series was canceled with each other. Therefore union among the recurrence plots, if the observed time series were embedded in sufficient high dimensions, remain information

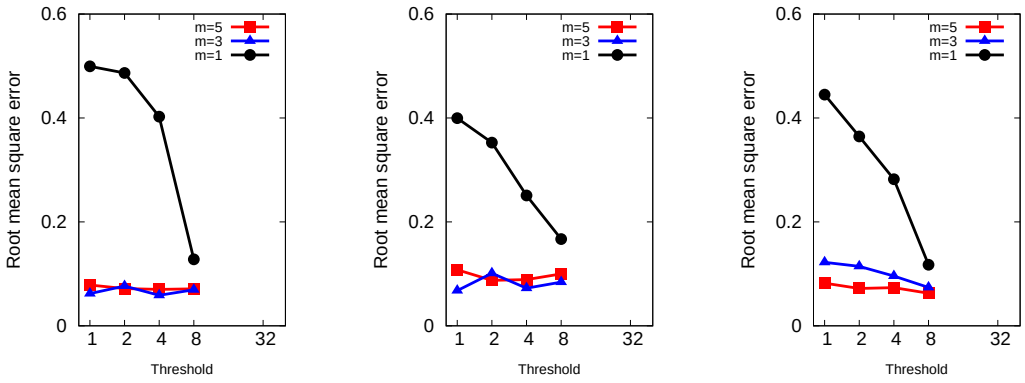

(a) RS, CH, and FS. $w = 500$. (b) CH, FS, and RS. $w = 500$. (c) FS, RS, and CH. $w = 500$.

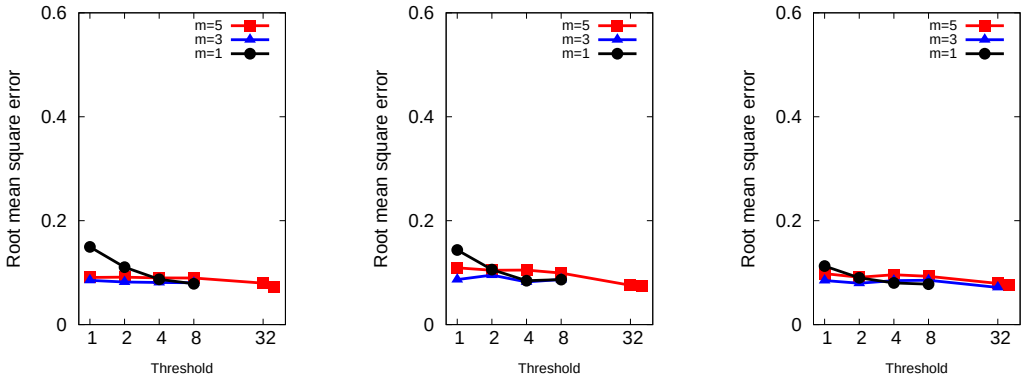

(d) RS, CH, and FS. $w = 1000$. (e) CH, FS, and RS. $w = 1000$. (f) FS, RS, and CH. $w = 1000$.

Figure 5.9: **Root mean square errors for combinations of Regular, Chattering, and Fast Spiking.**

of the common input. As Sauer [65] claimed based on Stark's version of embedding theorem, we would be able to reconstruct the time series of common input in case the forced system is deterministic and we can use responses of multiple forced system.

The results of this chapter confirmed that superposed recurrence plots can reconstruct the time series of the common input the even when we use a point process as the output of forced system. In other words, firing rates time series calculated within a width of time window can be used robustly for the reconstruction. The reconstructing method do not postulate any biological constrains derive from Izhikevich model and other models of neurons. Therefore, I conclude that proposed reconstructing method using superposed recurrence plots can be used for various time serious of point process in physics, biology, and psychology.

5.4 Reconstruction of common inputs using blink rates

The reconstructing method would be applied to the time series of blinking rates calculated as the numbers per unit time for reconstructing the time series of a common input. I therefore used this method to reconstruct the time series by using the the number of blinks per unit time reported in Chapter 2 and the such data of Ref. [3]. The first data obtained from the participants who had sufficient viewing experiences of Rakugo. The latter data obtained within two conditions: The blinks of participants who watched video of an expert actor and that watched a novice actor. These two actors performed the almost same story that shares the storyline and punchline. The performance durations were different each other because the novice performer had difficulty to act the full length of the story due to his performing skill.

The common input, in this situation, would correspond to the performance acted by the expert Rakugo performer. The time series of blinking rates were obtained from seven participants of experienced audience members, i.e., the targets of the observations in Chapter 2 because the degree of blink synchronization was highest in our reported data.

As shown in Fig. 5.10, temporal patterns in blinking rates differ with each audience members. Therefore, the recurrence plot of these blinking rates demonstrated the different patterns among them. However, several plots shared the common characteristics.

Figs. 5.11 and 5.12 showed that common white, i.e., unplotted area at around time index was 900 for Participants A, E, F, and G. As mentioned above, the recurrence plots of forced system are the subset of the common input. Thus, we can interpolate the loss of information using the union across the recurrence plots. I calculated superposed recurrence plot for reconstruct the common input. The embedding dimension was set to $m = 6$ as the sufficiently higher dimension for the driving system and the forced system while the accurate dimension was unknown. The time delay was set to $\tau = 6$ because the auto-correlation function of blinking rates showed almost minimal value in the delay.

Figure 5.14 demonstrates the results of the binarized superposed recurrence plots, i.e., estimated recurrence plots of the common input, for each threshold q. Using these binarized superposed recurrence plots, I reconstructed the time series of common inputs.

The reconstructed time series had fluctuations, indicating the common input vary in time. Especially, when the binarization threshold $q = 3$, large amplitude was appeared approximately at 1760 [s]. The time range corresponded to the white area in recurrence plots calculated using the blinking rates of respective audience members. Using these binarized superposed recurrence plots, I reconstructed the time series of common inputs.

Then, I applied the method the data in Ref. [3] as well. In this analysis, the embedding dimension was set to $m = 6$ as the sufficiently higher dimension for the driving system and the forced system while the accurate dimension was unknown. The time delay was set to $\tau = 6$ because the auto-correlation function of blinking rates showed almost minimal value in the delay.

Figure 5.15 and 5.16 demonstrate the superposed recurrence plots of the blink for participants who watched the expert and the novice actors. Dominant patterns were not detected in their visualizations. However, Fig. 5.17 shows the reconstructed common input for the data in Ref. [3]. In each time series, the amplitudes were larger in accordance with the binarization threshold while the tendencies were different each other. As shown in Fig. 5.17, the reconstructed time series of common input of the expert performance had several peaks in approximately $190 - 220$ [s]. Subsequently, it showed the relatively higher values over zero. In this scene, a character of the story finished off his drink. Participants would paid their attention for viewing this non-

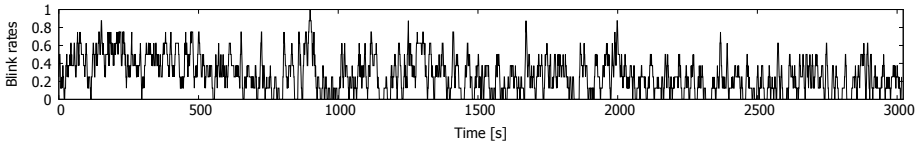

(a) Participants A

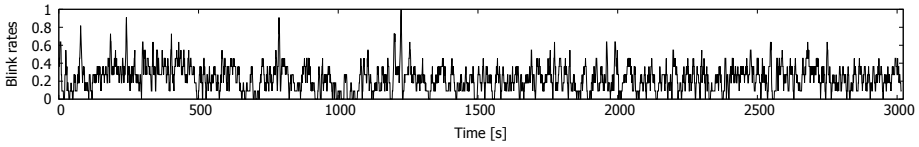

(b) Participants B

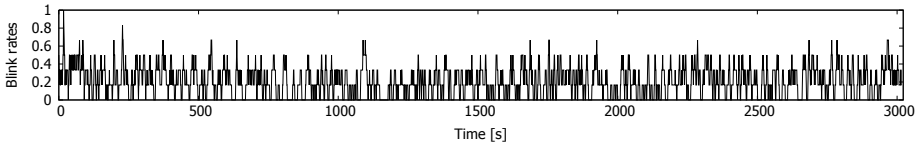

(c) Participants C

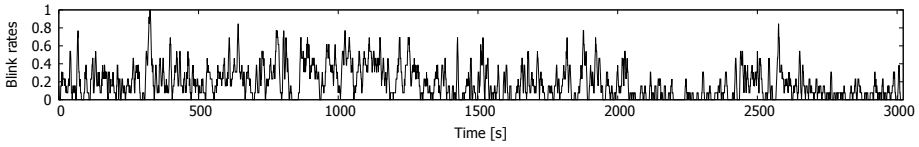

(d) Participants D

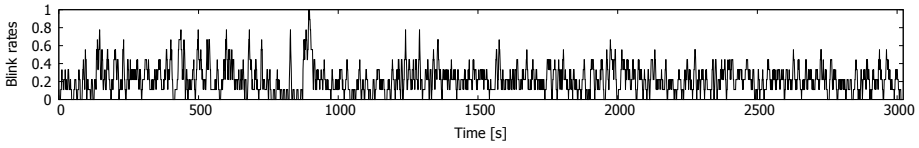

(e) Participants E

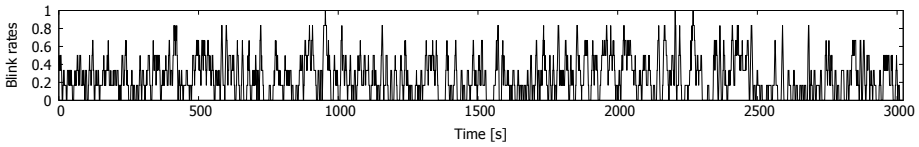

(f) Participants F

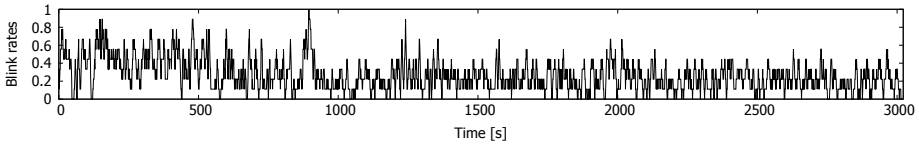

(g) Participants G

Figure 5.10: **Blinking rates of participants in a vaudeville setting**

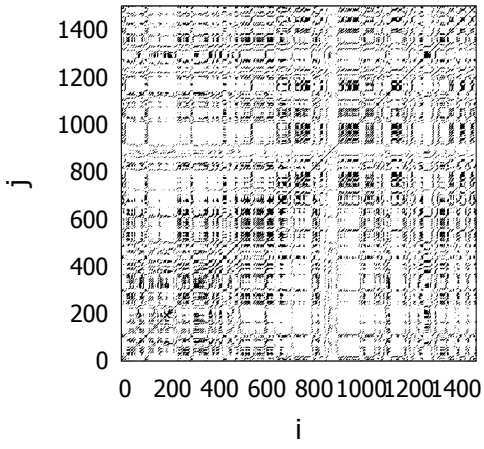

(a) Participants A

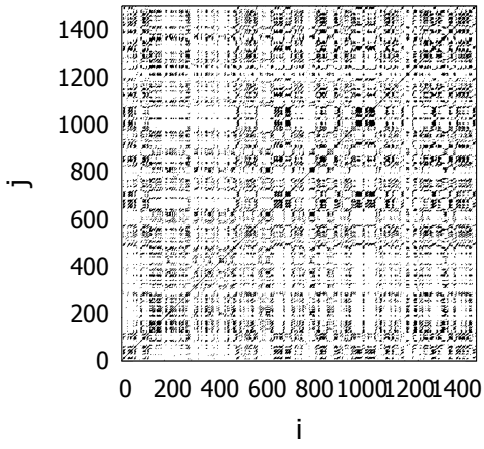

(b) Participants B

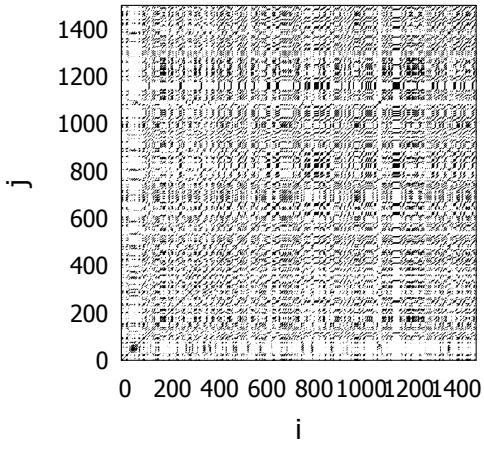

(c) Participants C

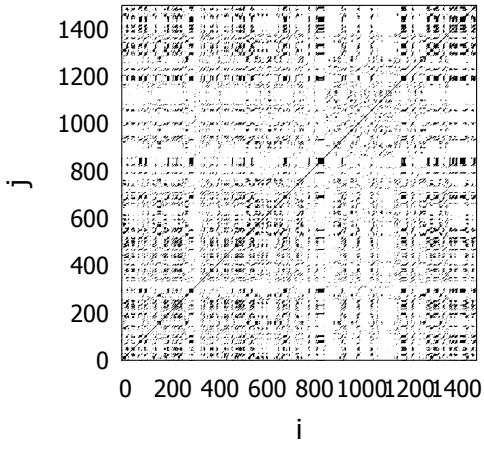

(d) Participants D

Figure 5.11: **Recurrence plots of the participants 1**

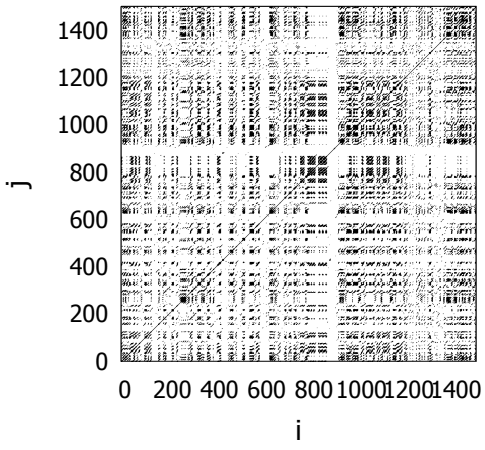

(a) Participants E

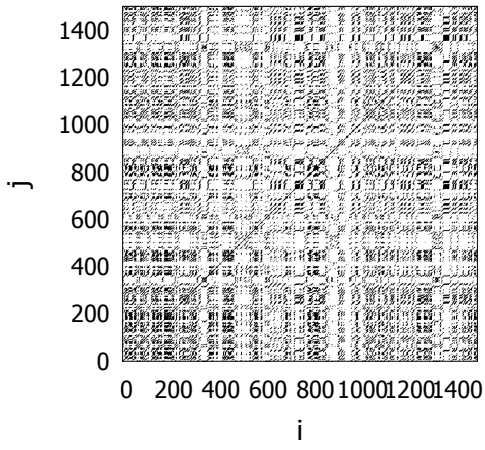

(b) Participants F

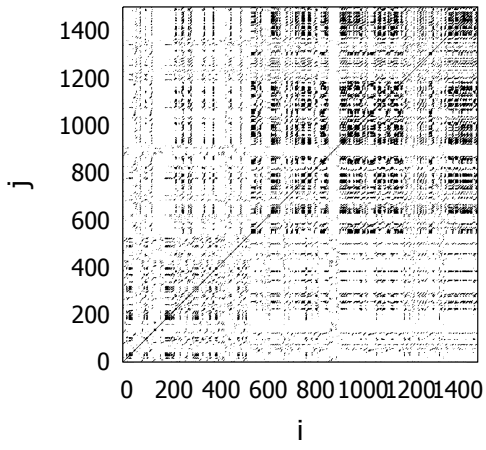

(c) Participants G

Figure 5.12: **Recurrence plots of the participants2**

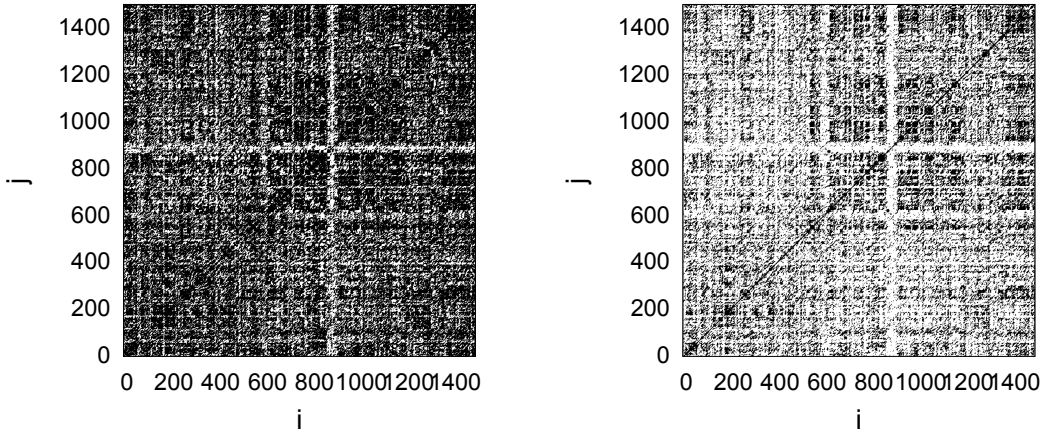

(a) $q = 1$

(b) $q = 2$

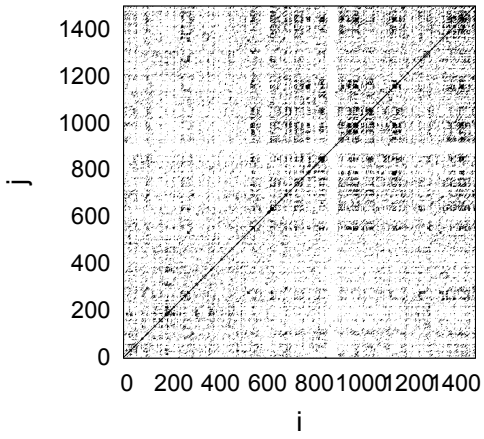

(c) $q = 3$

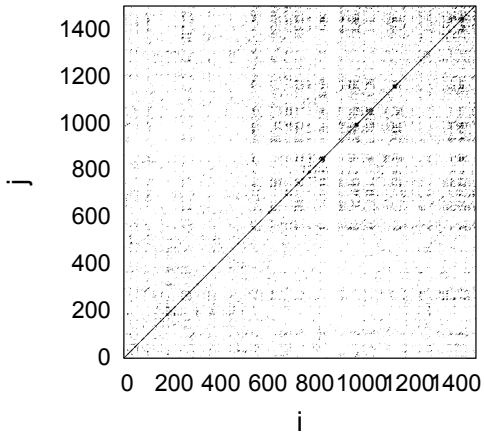

(d) $q = 4$

Figure 5.13: **Superposed recurrence plots for each binarizing threshold** q

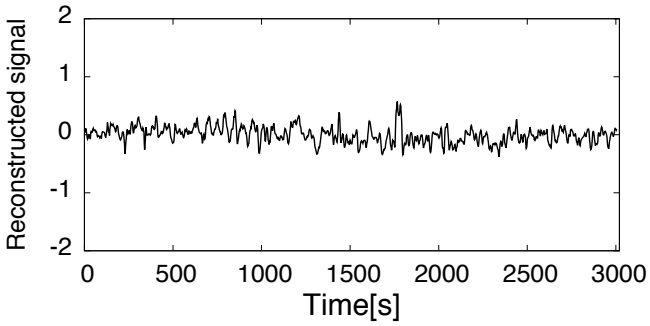

(a) $q = 1$

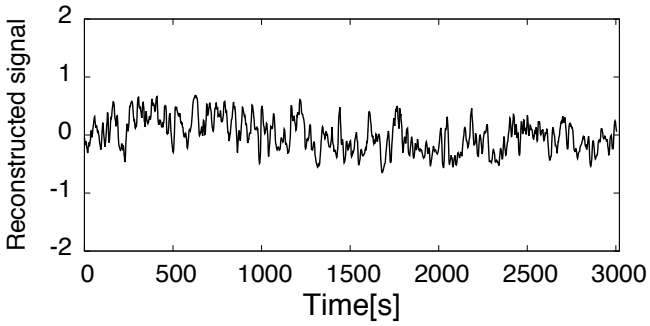

(b) $q = 2$

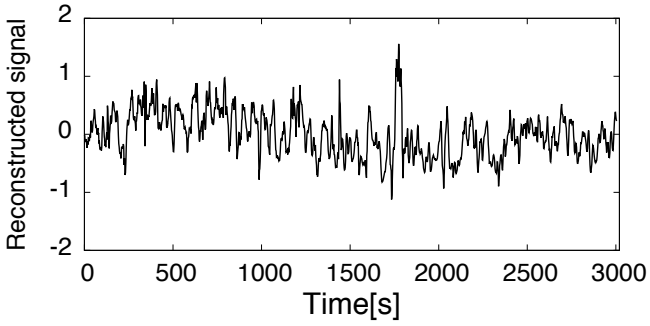

(c) $q = 3$

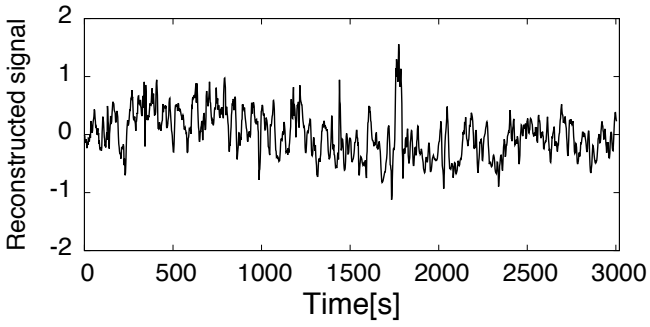

(d) $q = 4$

Figure 5.14: **Reconstructed time series using superposed recurrence plots for each binarizing threshold q**

linguistic expression and thus showed lower numbers of blinks. On the other hand, the reconstructed time series of common input of the novice performance former half of it showed in higher values. Then, the reconstructed time series demonstrated dominant lower peaks after 850 [s] and this tendency continue for approximately 100 [s] to the end of the story.

5.5 Discussion

5.5.1 Superposed recurrence plots for interpolation

For the calculations of these recurrence plots I only used the firing rates time series and did not use information of the common input. As shown in Fig. 5.4 shows the superposed recurrence plots, the rough shapes of these recurrence plots almost corresponded to recurrence plots of the common input. These results indicate that the reconstruction method in Ref. [2] could be applied to firing rates as well, as suggested by Ref. [66]. However, the patterns in these recurrence plots showed the dotted line in the recurrence plots of firing rates time series while the most of them were continuous lines in the recurrence plots of common input. Therefore, to reconstruct the common input, we must prepare multiple forced systems. By taking a union, the unique recurrences were cancelled with each other in the superposed recurrence plots.

The results of neurons with individual differences which respectively exhibit particular firing patterns (RS, CH, or FS) demonstrated that superposed recurrence plots calculated with using firing rates of Regular and Chattering Spiking neurons cannot reconstruct the common input when the time window is narrow (500[ms]) and the thresholds for binarization was too large. Moreover, precision of the reconstructed time series mainly depends on the embedding dimension m. If we do not embed the firing time series, i.e., $m = 1$, the shapes of the reconstructed time series are far from the common input, showing higher the root mean square errors. Since this tendency is found in all firing patterns, it is suggested that embedding is also necessary for the proposed reconstructing method [61].

When we used firing rates obtained from neurons of which firing patterns are different each other, the proposed superposed recurrence plots can reconstruct the time series of the common input as well. Superposed recurrence plots calculated by using first 27

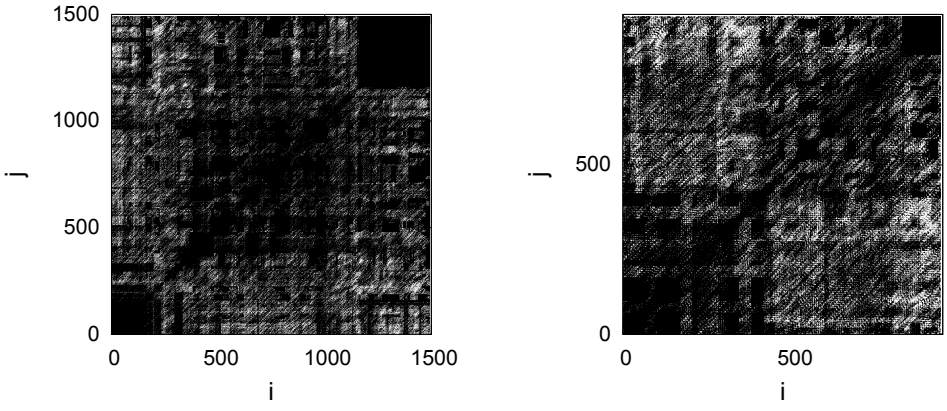

(a) $q = 1$

(b) $q = 1$

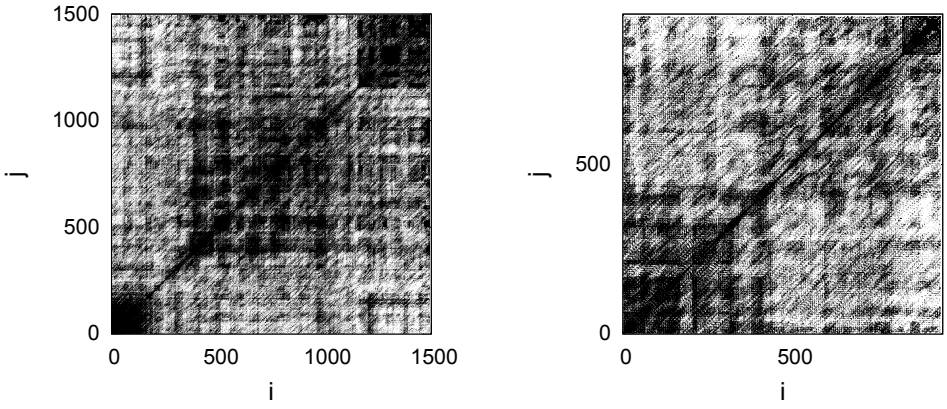

(c) $q = 2$

(d) $q = 2$

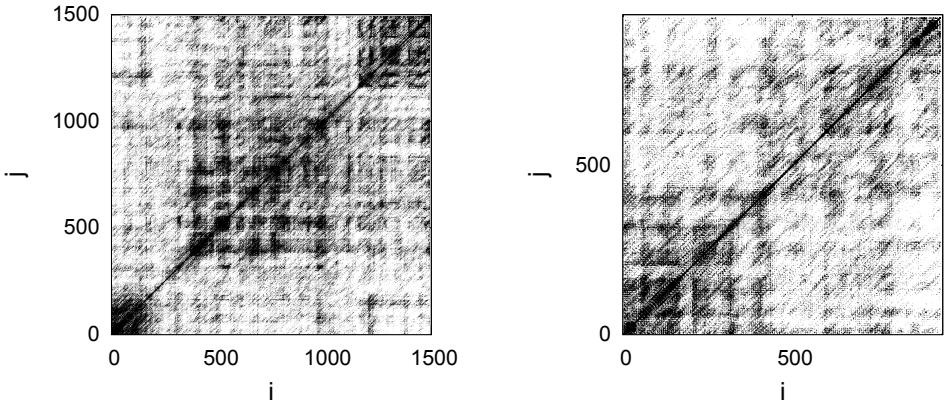

(e) $q = 3$

(f) $q = 3$

Figure 5.15: **Superposed recurrence plots for each binarizing threshold q (1)** Left panels show the recurrence plots of blinking data obtained from viewers of expert performance and right panels show that of novice performance.

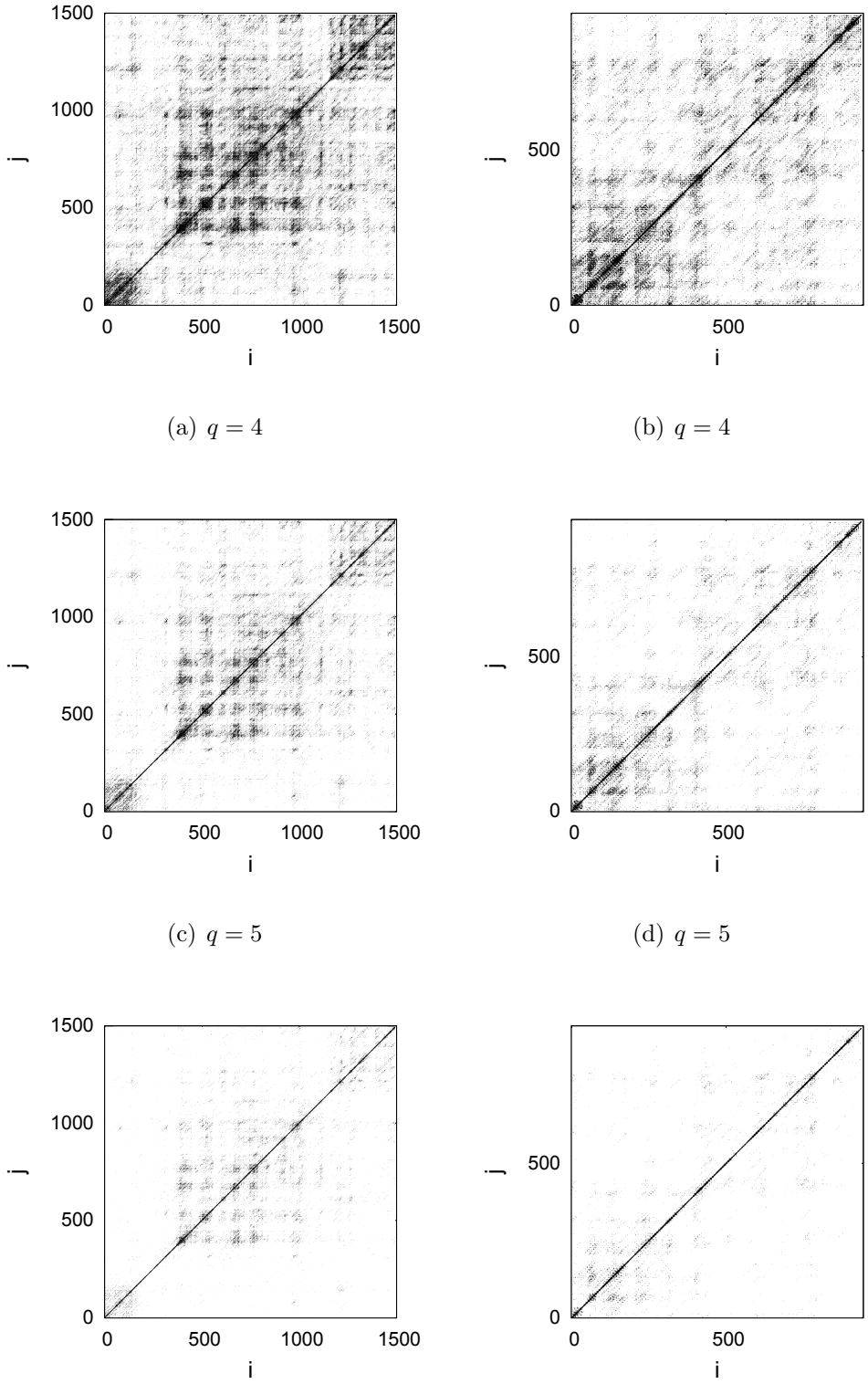

(a) $q = 4$

(b) $q = 4$

(c) $q = 5$

(d) $q = 5$

(e) $q = 6$

(f) $q = 6$

Figure 5.16: **Superposed recurrence plots for each binarizing threshold q (2)** Left panels show the recurrence plots of blinking data obtained from viewers of expert performance and right panels show that of novice performance.

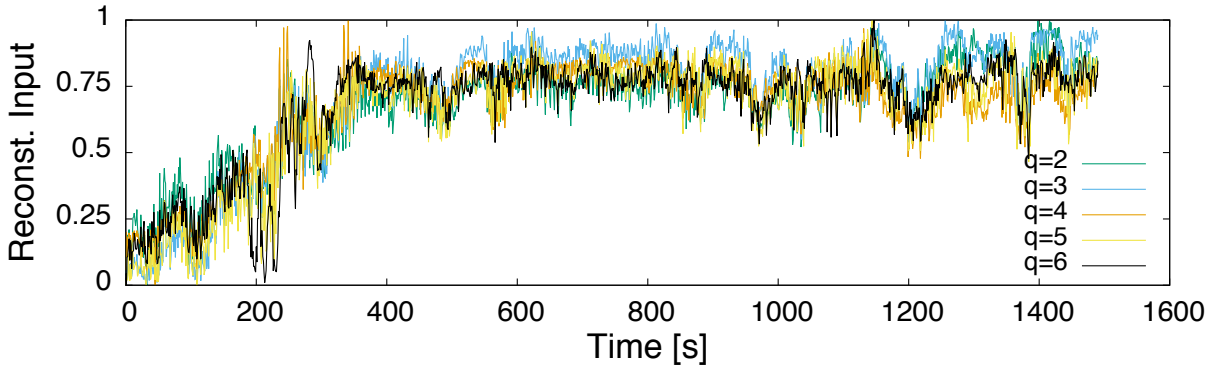

(a) Blink data obtained from vewers of expert performer

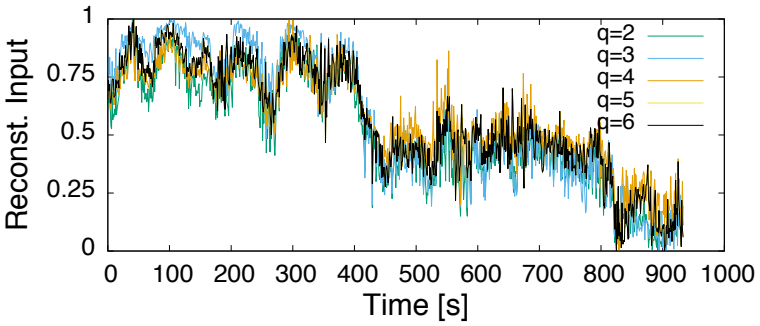

(b) Blinkind data obtained from vewers of novice performer

Figure 5.17: **Reconstructed time series using superposed recurrence plots for each binarizing threshold q for Ref. [3]**

Regular Spiking, middle 27 Chattering Spiking, and last 26 Fast Spiking models, out of 80 models, demonstrated the almost similar the recurrence plots to the recurrence plot calculated by using the common input. These results show that the rough shapes of the recurrence plots would be reproduced even if the baseline firing rates show differences in the order of several times. Moreover, the precisions of reconstructed time series were nearly independent on the threshold if the embedding dimension $m > 1$.

The method using superposed recurrence plot could reconstruct the common input even when we set lower threshold of binarization ($q = 1$). Although smooth lines are reconstructed if we used high threshold, we cannot obtain reconstructed time series when the threshold become much higher $q = 40(50\%)$ due to disappearance of the main lines and dots in the superposed recurrence plots. Because this trade off relationship have only little effects on the precision of reconstruction, we practically recommend the readers to use lower threshold that can certainly reconstruct the common input.

When I applied the method using superposed recurrence plots to the time series of human blinking rates, the time series that would correspond to the common input were reconstructed as well. In the first reconstructed time series, large amplitude was appeared approximately at 1760 [s]. In this time range, the expert performer acted a character who poured other characters a small cup of warmed sake (Japanese alcohol), with using salient the non-verbal expressions [42]. This scene located at the beginning of a drinking session after night-watch for preventing of fires in a cold night. Because this story develops with the interaction regarding sake after that, the scene has the role to introduce the latter half of this story to audience. In Fig. 5.14, there were no the salient fluctuations in the time series while the blinking rates of audience members were the averagely lower (Fig. 5.14). Therefore, the recurrences were observed in the embedded time delay coordinates, showing union of the recurrence plots corresponded to the common input rather than each forced blinking systems. To quantify the common input means to quantify the amplitude of the common input that drive the audience members' blinking system. The fact that the blinking systems recurred at the same time points indicates the forcing common input become had large amplitude at these points. Thus, the reconstructed amplitude of the common input would correspond to forcing power of actor's performance that attract attentions of the audience members.

The results of the comparison between the reconstructed input of the expert actor and that of the novice actor showed that the different variations while the almost same

stories were performed. The amplitude decreased for novice video in the last of the story. From the viewpoints of expertising level, the results suggest that the novice performer had lower skills and thus the it cannot attract participants' attentions in the end of the story. Therefore, the participants would have eyestrain and become lower concentrations. Regarding the participants who viewed the expert performance, the fluctuations of the reconstructed time series of the common input roughly corresponded to that of mean numbers of blinks. However, regarding those who viewed the novice performance, this tendency was not supported. Normalization of the time series, from zero to one, may enlarge the amplitude of the novice performer's common input. In both cases, the short-term fluctuations may relate to the respective expression of the performance. Thus, to reveal what is the dominant component of the common input, correlation analyses between the reconstructed time series of common input in this thesis and the performer's expressions, including linguistic, non-linguistic, and para-linguistic information, would be performed in the future research. If the analyses demonstrate the dominant component of the common input, reconstruction of common input based on superposed recurrence plot would be an assessment tool of the performance of which expressions keep audience members' attention.

5.5.2 Advantages of superposed recurrence plots and future research

As the results demonstrated, the differences in firing patterns (RS, CH, and FS) had little effect to the reconstruction. In addition to this, we can reconstruct with high precision although the firing patterns had different baseline firing rates. Because the reconstructing method is based on the common recurrences in the phase space, it is tolerant for outlier. In addition to this, these results indicate that our proposed method can detect a type of synchronization that "increase of firing numbers of multiple neurons that commonly driven by an input" by taking a union of recurrence plots. In the biological system, there exist synchronizations in broader sense other than accurate coincidences of firing of neurons that is describe by mathematical models. The proposed method can reconstruct the time series of a common input when forced neurons had individual differences and those neurons were mixed. Thus, this method would be applied to detect these synchronizations regardless of the baseline firing rates.

Results in this chapter were obtained when no noise was added on Izhikevich neuron models and the driving Duffing equation. However, time series of biological system in the real experimental data usually contains noises. Thus, for wider applications, to examine the precisions of the reconstructing method when we add dynamical noise to the driving or forcing systems as well as the observational noise would be issues of future study.

5.6 Conclusion

In this chapter, we first reviewed the methods for reconstruction of common input time series by using recurrence plots. Then, we proposed a reconstructing method using superposed recurrence plots of point process time series. The results demonstrated that this method can reconstruct the time series of the common input by embedding the time series of forced dynamical systems to a delay time coordinate, while the precision depends on the width of window size for firing rates calculation. The proposed reconstructing method using superposed recurrence plots could be widely applied for the point process data other than firing rates. Biological systems receive various common inputs, yet direct observation often changes behaviors of observed biological system. This method would be expected to estimation of common inputs based on the occurrence numbers biological signals as well as human behaviors.

In this chapter, I applied the method to the blinking numbers obtained from audience members who viewed vaudeville performances. The comparison between the expert's and novice's act suggest that the reconstructed common input would correspond to the expressions of performance. Thus, this reconstructing method would be also used for describing the life-long changes of a performance and comparing among several performers from the viewpoint of appealing powers as the amplitudes of common input. The quantification of the common input would provide researchers a path to scientific study on the expertising of performers.

Chapter 6

General Discussion

Throughout this thesis, the nature of blink synchronization in theatre was revealed. In the vaudeville settings, compared to the individual laboratory experiments, the degrees of the blink synchronizations were improved $30 - 60$ %. This result suggests that interactions among audience members facilitate blink synchronization in theatre. I would refer this accelerated effect is induced by inter-spectator force as the analogy of inter-molecular force although the medium of the synchronization is still unknown.

The observed attractive forces for blink synchronization were more intense for first-time viewers than frequent viewers. Moreover, for first-time viewers, the observed effects were significant through the performance. For frequent viewers, meanwhile, the observed effects were significant only for latter part of the performance. These results indicate that, in actual vaudeville settings, first-time viewers' inter-spectator forces have stronger influence on blink synchronizations than frequent viewers' the effect. Thus, attractive force has stronger influence than knowledge of the performance and the performer. However, for frequent viewers, the degree of blink synchronization increased as the performance progressed. The force seems to facilitate blink synchronization generally whereas the degree of the effect is depending on the viewing experience of audience members.

As the results of an experiment with individual participants, it is demonstrated that blink synchronizations could be established just by receiving a common input of expert performance. The theoretical and numerical researches have revealed that synchronization induced by a common input is not always maintained when oscillators mutually coupled [36]. However, in this thesis, blink synchronization was facilitated

in the situation where the audience members interact each other. Regarding blink synchronization in theatre, I conclude that the inter-spectator force would serve as an attractive force. Therefore, blink synchronizations would emerge in theatre are induced by the synergy of inputs from a performer and inter-spectator forces.

The computational approach study provided a more rigorous interpretation about the human spontaneous blinking and make us possible to predict trimodal distributions of IBI that have not been reported. These studies could lead a perspective that blink synchronizations emerges driven by inputs imposed by expressions of a performer. With considering the results of Izhikevich neuron model, I conclude that the common input could be reconstructed by using the mean blinking rates.

Blink synchronization would be achieve because the human blinking system has flexibility to shift within a short period from any states to a particular state where rapid serial blinks could occur. Such flexible shifts suggest the existence of temporally-localized nonlinearity in blinking system, resulting intermittently blinking and various IBI distributions. In theatre, one of the most influential driving input would be expressions of a performer. However, a blink generator receives individual's internal states, e.g., memory and emotion, or external stimulation, e.g., laughter from the surrounding audience members. As the results, blinking behaviours showed larger individual differences in the natural settings that allow participants to enjoy Rakugo performance as reported in this thesis. Nonetheless, the reconstruction method would be capable to estimate the amplitude of such common input from the blinking patterns of audience members because the method is less dependent on the baseline blinking rates.

In this thesis, albeit the inter-spectator force contributes to blink synchronization attractively, it is unrevealed that interactions among forced system facilitate synchronizations under the general situations where the forced systems receive a common input. Further computational researches are necessary for rigid findings. These challenges would provide a better understanding of blink synchronization in theatre as well.

Acknowledgment

I deeply appreciate Prof. Tohru Ikeguchi who has provided encouragements and supports throughout research in Graduate School of Engineering, Tokyo University of Science. I wish to express my appreciation to Prof. Kozo Fujii, Prof. Hitoshi Watanabe, Prof. Hiroyuki Yashima, Prof. Yukinobu Taniguchi, Prof. Osamu Araki, Prof. Mikio Hasegawa, and Prof. Hiroshi Gotoda for the fair and significant examination as my doctorate dissertation committee in Tokyo University of Science.

Prof. Kenji Morita also kindly provided the opportunity for me to study as a graduate student while I am an assistant professor of his research project in The University of Tokyo. I am very grateful to Prof. Kantaro Fujiwara and Dr. Yutaka Shimada who often have discussed human blinking in vaudeville settings form the viewpoints of neurological science and network science throughout my writing of this thesis. Prof. Takeshi Okada deepen the ideas of blink synchronization in vaudeville settings from the viewpoint of empirical studies on performing arts. Dr. Ying-Zong Liang gave advises especially on my source code of $D^{intervals}$ and kernel density estimation. I furthermore appreciate all members of the Nonlinear Problem Workshop for their useful comments and powerful encouragements. Thank you to all colleagues and friends in Tokyo University of Science and The University of Tokyo for their supports.

All experiments described in this thesis were realized by great cooperations by professional story-telling performers, Sanza Yanagiya, Bungiku Kokontei, Shosho Shumputei, Miyaji Katsura, and Koharu Tatekawa. I would thank to all other performers, theatre relations, and the audience members who participated in the experiments.

Bibliography

[1] Jonathan D Victor and Keith P Purpura. Metric-space analysis of spike trains: theory, algorithms and application. *Network: computation in neural systems*, 8(2):127–164, 1997.

[2] Yoshito Hirata, Shunsuke Horai, and Kazuyuki Aihara. Reproduction of distance matrices and original time series from recurrence plots and their applications. *The European Physical Journal Special Topics*, 164(1):13–22, 2008.

[3] R Nomura and T Okada. Spontaneous synchronization of eye-blinks during storytelling performance. *Cognitive Studies: Bulletin of the Japanese Cognitive Science Society*, 21(2):226–244, 2014.

[4] Eric Ponder and WP Kennedy. On the act of blinking. *Quarterly Journal of Experimental Physiology: Translation and Integration*, 18(2):89–110, 1927.

[5] FN Hoogeboom, AY Pogromsky, and H Nijmeijer. Huygens' synchronization: Experiments, modeling, and local stability analysis. *IFAC-PapersOnLine*, 48(18):146–151, 2015.

[6] James Pantaleone. Synchronization of metronomes. *American Journal of Physics*, 70(10):992–1000, 2002.

[7] Yuji Ikegaya, Gloster Aaron, Rosa Cossart, Dmitriy Aronov, Ilan Lampl, David Ferster, and Rafael Yuste. Synfire chains and cortical songs: temporal modules of cortical activity. *Science*, 304(5670):559–564, 2004.

[8] Michael J Richardson, Kerry L Marsh, Robert W Isenhower, Justin RL Goodman, and Richard C Schmidt. Rocking together: Dynamics of intentional and unintentional interpersonal coordination. *Human movement science*, 26(6):867–891, 2007.

[9] Robert R Provine. Yawns, laughs, smiles, tickles, and talking: Naturalistic and laboratory studies of facial action and social communication. *The psychology of facial expression*, pages 158–175, 1997.

[10] Ivan Norscia and Elisabetta Palagi. Yawn contagion and empathy in homo sapiens. *PloS one*, 6(12):e28472, 2011.

[11] Tamami Nakano, Yoshiharu Yamamoto, Keiichi Kitajo, Toshimitsu Takahashi, and Shigeru Kitazawa. Synchronization of spontaneous eyeblinks while viewing video stories. *Proceedings of the Royal Society of London B: Biological Sciences*, page rspb20090828, 2009.

[12] Renato E Mirollo and Steven H Strogatz. Synchronization of pulse-coupled biological oscillators. *SIAM Journal on Applied Mathematics*, 50(6):1645–1662, 1990.

[13] Jun-nosuke Teramae and Dan Tanaka. Robustness of the noise-induced phase synchronization in a general class of limit cycle oscillators. *Physical review letters*, 93(20):204103, 2004.

[14] Marc Sestir and Melanie C Green. You are who you watch: Identification and transportation effects on temporary self-concept. *Social Influence*, 5(4):272–288, 2010.

[15] Tom Van Laer, Ko De Ruyter, Luca M Visconti, and Martin Wetzels. The extended transportation-imagery model: A meta-analysis of the antecedents and consequences of consumers' narrative transportation. *Journal of Consumer research*, 40(5):797–817, 2013.

[16] David S Miall and Don Kuiken. Aspects of literary response: A new questionnaire. *Research in the Teaching of English*, pages 37–58, 1995.

[17] Ryota Nomura. Construction of a transportive experience scale for rakugo performance. *Japanese Journal of Laughter and Humor Research*, 20:32–43, 2013.

[18] Arthur Hall. The origin and purposes of blinking. *The British Journal of Ophthalmology*, 29(9):445–467, 1945.

[19] Tamami Nakano and Shigeru Kitazawa. Eyeblink entrainment at breakpoints of speech. *Experimental brain research*, 205(4):577–581, 2010.

[20] Teun Adrianus Van Dijk, Walter Kintsch, and Teun Adrianus Van Dijk. Strategies of discourse comprehension. 1983.

[21] P. N. Johnson-Laird. *Mental Models: Towards a Cognitive Science of Language, Inference, and Consciousness*. Harvard University Press, Cambridge, MA, USA, 1983.

[22] Rolf A Zwaan, Joseph P Magliano, and Arthur C Graesser. Dimensions of situation model construction in narrative comprehension. *Journal of experimental psychology: Learning, memory, and cognition*, 21(2):386, 1995.

[23] Gabriel A Radvansky and David E Copeland. Working memory and situation model updating. *Memory & Cognition*, 29(8):1073–1080, 2001.

[24] Zachary F Mainen and Terrence J Sejnowski. Reliability of spike timing in neocortical neurons. *Science*, 268(5216):1503–1506, 1995.

[25] Ryota Nomura and Shunichi Maruno. Constructing a coactivation model for explaining humor elicitation. *Psychology*, 2(5):477–485, 2011.

[26] Hidekazu Osanai and Hitoshi Okada. Construction of the literary response questionnaire for japanese. *The Japanese Journal of Psychology*, 82(2):167–174, 2011.

[27] Yoshinobu Kanda. Investigation of the freely available easy-to-use software eezrffor medical statistics. *Bone marrow transplantation*, 48(3):452–458, 2013.

[28] Amanda B Diekman and Sarah K Murnen. Learning to be little women and little men: The inequitable gender equality of nonsexist children's literature. *Sex Roles*, 50(5-6):373–385, 2004.

[29] Melanie C Green and Timothy C Brock. The role of transportation in the persuasiveness of public narratives. *Journal of personality and social psychology*, 79(5):701–721, 2000.

[30] Ryota Nomura and Shunichi Maruno. An integration of humor generation theories and a proposal of dynamical comprehension and elaboration theory. *Japanese Psychological Review*, 51(4):500–525, 2008.

[31] Kyosuke Fukuda and Katsuya Matsunaga. Changes in blink rate during signal discrimination tasks. *Japanese Psychological Research*, 25(3):140–146, 1983.

[32] Ryota Nomura, Kojun Hino, Makoto Shimazu, Yingzong Liang, and Takeshi Okada. Emotionally excited eyeblink-rate variability predicts an experience of transportation into the narrative world. *Frontiers in Psychology*, 6:447, 2015.

[33] Jihoon Oh, So-Yeong Jeong, and Jaeseung Jeong. The timing and temporal patterns of eye blinking are dynamically modulated by attention. *Human movement science*, 31(6):1353–1365, 2012.

[34] Morris K Holland and Gerald Tarlow. Blinking and thinking. *Perceptual and motor skills*, 41(2):403–406, 1975.

[35] Jihoon Oh, Mookyung Han, Bradley S Peterson, and Jaeseung Jeong. Spontaneous eyeblinks are correlated with responses during the stroop task. *PLoS One*, 7(4):e34871, 2012.

[36] Steven H Strogatz. *Nonlinear Dynamics and Chaos: With Applications to Physics, Biology, Chemistry, and Engineering*. CRC Press, 2014.

[37] Yuriy Brun, Giovanna Di Marzo Serugendo, Cristina Gacek, Holger Giese, Holger Kienle, Marin Litoiu, Hausi Müller, Mauro Pezzè, and Mary Shaw. Engineering self-adaptive systems through feedback loops. In *Software engineering for self-adaptive systems*, pages 48–70. Springer, 2009.

[38] Frank D Macías-Escrivá, Rodolfo Haber, Raul Del Toro, and Vicente Hernandez. Self-adaptive systems: A survey of current approaches, research challenges and applications. *Expert Systems with Applications*, 40(18):7267–7279, 2013.

[39] Rachel Rac-Lubashevsky, Heleen A Slagter, and Yoav Kessler. Tracking real-time changes in working memory updating and gating with the event-based eye-blink rate. *Scientific Reports*, 7(1):2547, 2017.

[40] David Hoppe, Stefan Helfmann, and Constantin A Rothkopf. Humans quickly learn to blink strategically in response to environmental task demands. *Proceedings of the National Academy of Sciences*, page 201714220, 2018.

[41] Kiyoshi Hoshino. Omstein-uhlenbeck first-passage-time models for spontaneous eye blinking. In *Engineering in Medicine and Biology Society, 1996. Bridging Disciplines for Biomedicine. Proceedings of the 18th Annual International Conference of the IEEE*, volume 5, pages 1784–1785. IEEE, 1996.

[42] Ryota Nomura, Yingzong Liang, and Takeshi Okada. Interactions among collective spectators facilitate eyeblink synchronization. *PloS ONE*, 10(10):e0140774, 2015.

[43] Timoleon Moraitis and Arko Ghosh. Withdrawal of voluntary inhibition unravels the off state of the spontaneous blink generator. *Neuropsychologia*, 65:279–286, 2014.

[44] Tamami Nakano, Makoto Kato, Yusuke Morito, Seishi Itoi, and Shigeru Kitazawa. Blink-related momentary activation of the default mode network while viewing videos. *Proceedings of the National Academy of Sciences*, 110(2):702–706, 2013.

[45] Michael Schindler, Peter Talkner, and Peter Hänggi. Firing time statistics for driven neuron models: analytic expressions versus numerics. *Physical Review Letters*, 93(4):048102, 2004.

[46] Anthony N Burkitt. A review of the integrate-and-fire neuron model: I. homogeneous synaptic input. *Biological Cybernetics*, 95(1):1–19, 2006.

[47] Leon Glass. Synchronization and rhythmic processes in physiology. *Nature*, 410(6825):277–284, 2001.

[48] Benjamin Lindner and Lutz Schimansky-Geier. Transmission of noise coded versus additive signals through a neuronal ensemble. *Physical Review Letters*, 86(14):2934–2937, 2001.

[49] Magnus JE Richardson. Firing-rate response of linear and nonlinear integrate-and-fire neurons to modulated current-based and conductance-based synaptic drive. *Physical Review E*, 76(2):021919, 2007.

[50] Jaime Kaminer, Alice S Powers, Kyle G Horn, Channing Hui, and Craig Evinger. Characterizing the spontaneous blink generator: an animal model. *Journal of Neuroscience*, 31(31):11256–11267, 2011.

[51] Antonio AV Cruz, Denny M Garcia, Carolina T Pinto, and Sheila P Cechetti. Spontaneous eyeblink activity. *The Ocular Surface*, 9(1):29–41, 2011.

[52] P. K. Janert. Kernel density estimation. 2008. Internet: https://metacpan.org/release/JANERT/Statistics-KernelEstimation-0.05.

[53] Nate Yoder. Peakfinder. 2011. Internet: http://www.mathworks.com/matlabcentral/fileexchange/25500.

[54] Bryant J Jongkees and Lorenza S Colzato. Spontaneous eye blink rate as predictor of dopamine-related cognitive function? a review. *Neuroscience & Biobehavioral Reviews*, 71:58–82, 2016.

[55] Careesa C Liu, Sujoy Ghosh Hajra, Teresa PL Cheung, Xiaowei Song, and Ryan CN D'Arcy. Spontaneous blinks activate the precuneus: characterizing blink-related oscillations using magnetoencephalography. *Frontiers in Human Neuroscience*, 11:489, 2017.

[56] Rufin VanRullen. Visual attention: a rhythmic process? *Current Biology*, 23(24):R1110–R1112, 2013.

[57] Luca Bonfiglio, Stefano Sello, Paolo Andre, Maria Chiara Carboncini, Pieranna Arrighi, and Bruno Rossi. Blink-related delta oscillations in the resting-state eeg: a wavelet analysis. *Neuroscience letters*, 449(1):57–60, 2009.

[58] Floris Takens. Detecting strange attractors in turbulence. In *Dynamical Systems and Turbulence, Warwick 1980*, pages 366–381. Springer, 1981.

[59] J-P Eckmann, S Oliffson Kamphorst, and David Ruelle. Recurrence plots of dynamical systems. *EPL (Europhysics Letters)*, 4(9):973, 1987.

[60] MC Casdagli. Recurrence plots revisited. *Physica D: Nonlinear Phenomena*, 108(1-2):12–44, 1997.

[61] Norbert Marwan, M Carmen Romano, Marco Thiel, and Jürgen Kurths. Recurrence plots for the analysis of complex systems. *Physics Reports*, 438(5-6):237–329, 2007.

[62] Gertrudis Hortensia González-Gómez, Oscar Infante, Paola Martínez-García, and Claudia Lerma. Analysis of diagonals in cross recurrence plots between heart rate and systolic blood pressure during supine position and active standing in healthy adults. *Chaos: An Interdisciplinary Journal of Nonlinear Science*, 28(8):085704, 2018.

[63] Daniel Angus and Janet Wiles. Social semantic networks: Measuring topic management in discourse using a pyramid of conceptual recurrence metrics. *Chaos: An Interdisciplinary Journal of Nonlinear Science*, 28(8):085723, 2018.

[64] Jaroslav Stark. Delay embeddings for forced systems. i. deterministic forcing. *Journal of Nonlinear Science*, 9(3):255–332, 1999.

[65] Timothy D Sauer. Reconstruction of shared nonlinear dynamics in a network. *Physical Review Letters*, 93(19):198701, 2004.

[66] Kantaro Fujiwara, Naruhiro Kurokawa, Taiji Yamada, and Tohru Ikeguchi. Detection of neuronal inputs using recurrence plots. *The Brain and Neural Networks*, 21(2):79–86, 2014.

[67] Eugene M Izhikevich. Simple model of spiking neurons. *IEEE Transactions on Neural Networks*, 14(6):1569–1572, 2003.

Publication

Peer reviewed papers

1. Threshold-varying integrate-and-fire model reproduces distributions of spontaneous blink intervals.
（閾値が変動する積分発火モデルは自発性瞬目間隔分布を再現する）
Ryota Nomura, Ying-Zong Liang, Kenji Morita, Kantaro Fujiwara, Tohru Ikeguchi.
PLoS ONE, 13(10) : e0206528. （2018 年 10 月）
DOI : 10.1371/journal.pone.0206528

2. Assessing the Appeal Power of Narrative Performance by using Eyeblink Synchronization among Audience.
（観客間の瞬目同期を用いた話芸における訴求力の評価）
Ryota Nomura, Takeshi Okada.
In Takashi Ogata & Taisuke Akimoto (Eds.), Computational and Cognitive Approaches to Narratology. Chapter11. pp. 311-328. PA : IGI Global. (2016 年)
DOI : 10.4018/978-1-5225-0432-0.ch011

3. Interactions among Collective Spectators Facilitate Eyeblink Synchronization.
（観客間の相互作用は瞬目同期を促進する）
Ryota Nomura, Yingzong Liang, Takeshi Okada.
PLoS ONE, 10(10): e0140774.（2015 年 10 月）
DOI : 10.1371/journal.pone.0140774

4. Emotionally excited eyeblink-rate variability predicts an experience of transportation into the narrative world
（感情を伴う瞬目率の変動は物語への没頭体験を予測する）
Ryota Nomura, Kojun Hino, Makoto Shimazu, Yingzong Liang, Takeshi Okada.
Frontiers in Psychology, Vol 6, Article 447, pp 1-10（2015 年 4 月）
DOI : 10.3389/fpsyg.2015.00447, 2015.

5. 話芸鑑賞時の自発的なまばたきの同期
野村 亮太，岡田 猛
認知科学，Vol. 21, No. 2, pp. 226-244.（2014 年 6 月）
DOI : 10.11225/jcss.21.226

6. Modeling of Human Spontaneous Eyeblinks
（ヒトの自発性瞬目のモデリング）Ryota Nomura, Tohru Ikeguchi.

2016 International Symposium on Nonlinear Theory and Its Applications, NOLTA2016，pp. 502-505. （2016 年 11 月）

National Conference Proceedings

1. 野村亮太, 池口徹 重畳リカレンスプロットを用いた共通入力の再構成, 電子情報通信学会 電子情報通信学会 2019 年総合大会, N-1-35, 2019
2. 野村亮太, 池口 徹, ジョイントリカレンスプロットによる瞬目同期の時間スケール解析, 電子情報通信学会 2018 年総合大会, N-1-24, 2018
3. 野村亮太, 教育場面での瞬目同期の定量評価 教育現場でもまばたきでコミュニケーションしよう！第 81 回日本心理学会, 2017（公募シンポジウム，話題提供者）
4. 野村亮太, 池口徹 三遊亭圓生の落語『死神』の非線形時系列解析, 電子情報通信学会 電子情報通信学会 2017 年ソサイエティ大会, N-1-25, 2017
5. 野村亮太, 大阪の笑いを探る―ぼけとつっこみ―, 日本パーソナリティ心理学会第 25 回大会 大会準備委員会・なにわ大阪の「笑い」に関する調査と研究プロジェクト共催シンポジウム, 2016 （指定討論者）. 話題提供者：森下伸也，藤田曜, 指定討論者：野村亮太, 総合討論者：森田亜矢子